ELSEVIER

Nuclear Physics A 589 (1995) 17–57

NUCLEAR PHYSICS A

Collective states of even–even and odd nuclei with β_2, β_3, ..., β_N deformations

V.Yu. Denisov, A.Ya. Dzyublik

Institute for Nuclear Research, Prospect Nauki 47, 252028 Kiev, Ukraine

Received 13 September 1994; revised 24 February 1995

Abstract

Simple analytic expressions are derived for the energies of vibrational–rotational bands both of positive and negative parity in soft nuclei with nonvanishing equilibrium deformations β_2^0, β_3^0, ..., β_N^0. Expressions for the reduced probabilities of E1, E2 and E3 transitions are derived. The calculated values of energies are in good agreement with experimental data for ^{144,146}Ba, ^{146}Ce, ^{146,148,150}Nd, ^{151}Pm, ^{150}Sm, ^{220,222}Rn, ^{217,219,221}Fr, ^{218,219,220,221,222,223,224,225,226,227,228}Ra, ^{219,223,225,227}Ac and ^{220,221,222,223,224,225,226,228,229}Th isotopes. The correlation between experimental and theoretical values of the branching ratio $B(\mathrm{E1}, I \to I-1)/B(\mathrm{E2}, I \to I-2)$ for some isotopes is satisfactory. The calculated values of the ratios $B(\mathrm{E1}, I \to I-1)/B(\mathrm{E1}, 1 \to 0)$, $B(\mathrm{E2}, I \to I-2)/B(\mathrm{E2}, 2 \to 0)$ and $B(\mathrm{E3}, I \to I-3)/B(\mathrm{E3}, 3 \to 0)$ are in satisfactory agreement with experimental data available for ^{226}Ra.

1. Introduction

Intensive experimental and theoretical studies of different phenomena in nuclei with equilibrium quadrupole and octupole deformations have been continuing during the last ten years [1–42]. The microscopic origin of equilibrium octupole deformation is connected with a strong coupling between single-particle states, which differ by $\Delta l = 3$ and/or $\Delta j = 3$ [3]. Two rotational bands of opposite parity have been observed in nuclei with quadrupole (β_2) and octupole (β_3) deformations [1,2,13–43]. Strong dipole transitions occur between rotational levels with opposite parity due to a polarization electric dipole moment [6–12] in these nuclei. This dipole moment is associated with electrostatic redistribution of protons relative to neutrons in the nuclear volume and on its surface [8–12]. Detailed discussions of the polarization electric dipole moment are presented in Refs. [1,2,4,6–12].

SSDI 0375-9474(95)00075-5

As a rule nuclei, having both equilibrium quadrupole and octupole deformations, have also equilibrium deformations of multipolarity $\lambda \geqslant 4$ [1,4,6,7]. The quadrupole and octupole deformations in these nuclei have close values and as a rule largest values [1,4,6,7].

These nuclei with nonzero deformations of odd multipolarities have reflection asymmetry, which is restored due to the tunneling transitions between shape states with opposite values of odd multipolarity deformations [8,11,12,44]. These nuclei have two symmetric minima of the potential energy, corresponding to opposite values of odd equilibrium deformations $\mp\beta_\lambda^0$. This leads to a double degeneracy of the levels, which is removed by tunneling transitions under potential barrier separating potential wells with opposite values of the odd deformation parameters. Due to the tunneling transitions in nuclei with deformations of odd multipolarities there are two opposite-parity rotational bands with equal K.

In previous studies a model of collective excitations of soft deformed even–even [13,14] and odd [15] nuclei having both quadrupole and octupole deformations is constructed. In these papers simple expressions for the energy levels of even and odd bands and for the reduced probabilities of electric dipole and quadrupole transitions are obtained. The calculations of E3 transitions are presented in Ref. [16].

The model proposed in Refs. [13–15] is a generalization of the Davydov–Chaban [45,46] model, which describes vibrational–rotational spectra of soft even–even nuclei only with a quadrupole deformation, on the case of nuclei with both quadrupole and octupole deformations. The calculations of the reduced probabilities for electromagnetic transitions have been done [13–16] in analogy with calculations [46,47] for nuclei with pure β_2 deformation.

One should note also papers [48–50] dealt with the vibrational–rotational spectra of soft even–even nuclei, having only octupole deformation, and paper [51] devoted to calculations of rotational bands of a rigid quadrupole rotor both of A and B_1, B_2, B_3 symmetry with respect to the group D_2.

Now we extend our model to the case of nuclei with $\beta_2, \beta_3, \ldots, \beta_N$ deformations. As we noted in Ref. [14] the deformations of higher multipolarities give significant contributions to reduced probabilities of dipole transitions in the soft-rotator model.

A simple expression for energies of the even–even nuclei with $\beta_2, \beta_3, \ldots, \beta_N$ deformations is derived in Section 2. An extension of these results to the case of odd nuclei is presented in Section 3. Limiting cases of rigid and very soft nuclei are considered in Section 4. Section 5 is devoted to calculations of electromagnetic transitions in such nuclei. In Section 6 the discussion of results and comparison with experimental data are presented.

2. Energy levels of even–even nuclei

The distance between the center of the deformed nucleus and its surface in the direction of the polar angles ϑ, φ in the laboratory frame x, y, z is given by the

expression [44,46]

$$R(\vartheta,\varphi) = R_0\left[1 + \sum_{\lambda\mu}\alpha_{\lambda\mu}Y^*_{\lambda\mu}(\vartheta,\varphi)\right], \tag{1}$$

where R_0 is the radius and $\alpha_{\lambda\mu}$ are the parameters of nuclear deformations. Let us introduce an intrinsic coordinate system with the origin at the center of mass and with axes ξ, η, ζ directed along the principal axes of inertia of the nucleus, whose orientation relative to the x-, y-, z-axes is defined by the eulerian angles $\theta = \{\theta_1, \theta_2, \theta_3\}$.

Next, we assume that the nuclei are rigid with respect to nonaxial deformations of the nuclear surface. In other words, we consider only axially symmetric deformations. Then

$$\alpha_{\lambda\mu} = \beta_\lambda D^\lambda_{0\mu}(\theta), \tag{2}$$

where β_λ are the deformation parameters in the intrinsic coordinate system, which vary in the interval $-\infty < \beta_\lambda < \infty$ for odd values of λ and $0 \leqslant \beta_\lambda < \infty$ for even ones, $D^\lambda_{0\mu}(\theta)$ is the Wigner function.

In order to dismiss the spurious shift of the center of mass of the nucleus with varying deformation of odd multipolarity we must introduce the dipole deformation by the relation [8,11,12]

$$\beta_1 = \frac{3}{2}\sqrt{\frac{3}{\pi}}\sum_{\lambda=2}^{N}\frac{\lambda+1}{\sqrt{(2\lambda+1)(2\lambda+3)}}\beta_\lambda\beta_{\lambda+1}. \tag{3}$$

Note that β_1 is an order of magnitude smaller than β_λ ($\lambda \geqslant 2$) deformations [11,44] and therefore may be neglected.

We shall consider only axially symmetric nuclei for which the hamiltonian can be shown to be

$$\widehat{H} = -\sum_{\lambda=2}^{N}\frac{\hbar^2}{2B_\lambda}\frac{1}{\beta_\lambda^3}\frac{\partial}{\partial\beta_\lambda}\beta_\lambda^3\frac{\partial}{\partial\beta_\lambda} + \frac{\hbar^2\widehat{I}^2}{\sum_{\lambda=2}^{N}\lambda(\lambda+1)B_\lambda\beta_\lambda^2} + V_0(\{\beta_\lambda\}), \tag{4}$$

where B_λ are the mass parameters, $\widehat{I}$ is the nuclear spin operator in units of $\hbar$, and $V_0(\{\beta_\lambda\})$ is the potential energy, $\{\beta_\lambda\} = \{\beta_2, \beta_3, \ldots, \beta_N\}$. For more simple cases of β_2 and β_3 deformations the hamiltonian is provided by Refs. [45–50].

The solution of the Schrödinger equation

$$\widehat{H}\Psi_I(\{\beta_\lambda\},\theta) = E_I\Psi_I(\{\beta_\lambda\},\theta) \tag{5}$$

is

$$\Psi_I^\pm(\{\beta_\lambda\},\theta) = (\beta_2\beta_3\cdots\beta_N)^{-3/2}\psi_I^\pm(\{\beta_\kappa\})|IM0\pm\rangle, \tag{6}$$

where the function $|IM0\pm\rangle$ describes the rotation of an axially symmetric nucleus with spin projections M onto the axis z and $K = 0$ onto the nuclear symmetry axis ζ. The

function with plus sign transforms in accordance with the irreducible representation A of the group D_2, whereas the function with the minus sign transforms according to the irreducible representation B_1. In the general case these functions have the form [44,46,51]

$$|IMK\pm\rangle = \sqrt{\frac{2I+1}{16\pi^2(1+\delta_{K0})}}\left(D^I_{KM}(\theta) \pm (-1)^I D^I_{-KM}(\theta)\right), \tag{7}$$

where $K = 0, 2, 4, \ldots$ and δ_{ij} is the Kronecker symbol. We restrict ourselves by the states with $K = 0$, for which $|IM0+\rangle \neq 0$ when $I = 0, 2, 4, \ldots$ and $|IM0-\rangle \neq 0$ when $I = 1, 3, 5, \ldots$. The functions $\psi^+(\{\beta_\lambda\})$ and $\psi^-(\{\beta_\lambda\})$ are, respectively, symmetric and antisymmetric with respect to reflection in the plane ξ, η, which is perpendicular to the symmetry axis ζ, i.e. $\psi^\pm(\{\beta_\lambda\}) = \pm\psi^\pm(\{(-1)^\lambda\beta_\lambda\})$. Therefore, the functions $\psi^+(\{\beta_\lambda\})$ and $\psi^-(\{\beta_\lambda\})$ describe states of positive and negative parity, respectively. The form (6) of the wave function for even–even nuclei is a result of equivalence of reflection $\beta_\lambda \to (-1)^\lambda\beta_\lambda$ to rotation around the axis perpendicular to the symmetry axis ζ (see also Ref. [44]).

From (4)–(6) we obtain the equation for $\psi^\pm_I(\{\beta_\lambda\})$:

$$\left[-\sum_{\lambda=2}^{N}\frac{\hbar^2}{2B_\lambda}\frac{\partial^2}{\partial\beta_\lambda^2} + \frac{\hbar^2 I(I+1)}{\sum_{\lambda=2}^{N}\lambda(\lambda+1)B_\lambda\beta_\lambda^2} + V(\{\beta_\lambda\}) - E_I\right]\psi^\pm_I(\{\beta_\lambda\}) = 0, \tag{8}$$

where

$$V(\{\beta_\lambda\}) = V_0(\{\beta_\lambda\}) + \tfrac{3}{8}\hbar^2\sum_{\lambda=2}^{N}\frac{1}{B_\lambda\beta_\lambda^2}. \tag{9}$$

Introducing reduced deformation parameters

$$\tilde\beta_\lambda = (B_\lambda/B)^{1/2}\beta_\lambda \tag{10}$$

with

$$B = (B_2 + B_3 + \cdots + B_N)/(N-1), \tag{11}$$

we rewrite Eq. (8) in more symmetric form

$$\left[-\frac{\hbar^2}{2B}\Delta + \frac{\hbar^2 I(I+1)}{B\tilde\beta^2\sum_{\lambda=2}^{N}\lambda(\lambda+1)\left(\tilde\beta_\lambda/\tilde\beta\right)^2} + V(\{\tilde\beta_\lambda\}) - E_I\right]\psi^\pm_I(\{\tilde\beta_\lambda\}) = 0, \tag{12}$$

where Δ is the laplacian operator,

$$\Delta = \frac{\partial^2}{\partial\tilde\beta_2^2} + \frac{\partial^2}{\partial\tilde\beta_3^2} + \cdots + \frac{\partial^2}{\partial\tilde\beta_N^2}, \tag{13}$$

$\tilde\beta$ is the length of the vector $\{\tilde\beta_2, \tilde\beta_3, \ldots, \tilde\beta_N\}$ in $(N-1)$-dimensional space,

$$\tilde\beta = \left[\tilde\beta_2^2 + \tilde\beta_3^2 + \cdots + \tilde\beta_N^2\right]^{1/2}. \tag{14}$$

Now we introduce in this space the spherical coordinates $\vartheta_1, \vartheta_2, \vartheta_3, \ldots, \vartheta_{N-2}$ by

$$\begin{aligned}
\widetilde{\beta}_2 &= \widetilde{\beta} \sin\vartheta_{N-2} \cdots \sin\vartheta_2 \sin\vartheta_1, \\
\widetilde{\beta}_3 &= \widetilde{\beta} \sin\vartheta_{N-2} \cdots \sin\vartheta_2 \cos\vartheta_1, \\
&\cdots, \\
\widetilde{\beta}_{N-1} &= \widetilde{\beta} \sin\vartheta_{N-2} \cos\vartheta_{N-3}, \\
\widetilde{\beta}_N &= \widetilde{\beta} \cos\vartheta_{N-2}.
\end{aligned} \tag{15}$$

They vary in the following limits:

$$\begin{aligned}
&0 \leqslant \widetilde{\beta} < \infty, \qquad 0 \leqslant \vartheta_1 < 2\pi, \\
&0 \leqslant \theta_\kappa < \pi, \qquad \kappa \neq 1.
\end{aligned} \tag{16}$$

Then (12) takes the form

$$\begin{aligned}
&\left[-\frac{\hbar^2}{2B} \left(\frac{1}{\widetilde{\beta}^{N-2}} \frac{\partial}{\partial \widetilde{\beta}} \widetilde{\beta}^{N-2} \frac{\partial}{\partial \widetilde{\beta}} + \frac{1}{\widetilde{\beta}^2} \Delta_\vartheta \right) + \frac{\hbar^2 I(I+1)}{6B\mathcal{F}(\{\vartheta_\kappa\})\widetilde{\beta}^2} + V(\widetilde{\beta}, \{\vartheta_\kappa\}) - E_I \right] \\
&\quad \times \psi_I^{\pm}(\{\beta_\lambda\}) = 0,
\end{aligned} \tag{17}$$

where Δ_ϑ is the angular part of the laplacian operator [55]

$$\Delta_\vartheta = \frac{1}{\sin^{N-3}\vartheta_{N-2}} \frac{\partial}{\partial\vartheta_{N-2}} \sin^{N-3}\vartheta_{N-2} \frac{\partial}{\partial\vartheta_{N-2}} + \cdots + \frac{1}{\sin^2\vartheta_{N-2} \cdots \sin^2\vartheta_2} \frac{\partial^2}{\partial\vartheta_1^2}, \tag{18}$$

and

$$\mathcal{F}(\{\vartheta_\kappa\}) = \tfrac{1}{6} \sum_{\lambda=2}^{N} \lambda(\lambda+1) \left(\frac{\widetilde{\beta}_\lambda}{\widetilde{\beta}} \right)^2. \tag{19}$$

The factor $\mathcal{F}(\{\vartheta_\kappa\})$ varies in the limits $1 \leqslant \mathcal{F} \leqslant \frac{1}{6}N(N+1)$. The value $\mathcal{F} = 1$ corresponds to pure quadrupole deformation of the nucleus, and $\mathcal{F} = \frac{1}{6}N(N+1)$ to the pure β_N one.

The normalization constraint for the wave function modifies as

$$\begin{aligned}
&\int \left| \psi_I^{\pm}(|\{\beta_\lambda|\}) \right|^2 \mathrm{d}\beta_2 \, \mathrm{d}\beta_3 \cdots \beta_N = \\
&\quad \left(\frac{B_2 B_3 \cdots B_N}{B^{N-1}} \right)^{1/2} \int \left| \psi_I^{\pm}(|\widetilde{\beta}, \{\vartheta_\kappa\}) \right|^2 \widetilde{\beta}^{N-2} \, \mathrm{d}\widetilde{\beta} \, \mathrm{d}\Omega = 1, \\
&\mathrm{d}\Omega = \sin^{N-3}\vartheta_{N-2} \, \mathrm{d}\vartheta_{N-2} \cdots \sin\vartheta_2 \, \mathrm{d}\vartheta_2 \, \mathrm{d}\vartheta_1.
\end{aligned} \tag{20}$$

The potential energy has two minima with coordinates β_λ^0 and $\beta_\lambda'^0 = (-1)^\lambda \beta_\lambda^0$. They correspond to nuclear shapes, which coincide as a result of the reflection in the plane ξ, η, corresponding to the transformation

$$\widetilde{\beta}^0, \{\vartheta_\kappa^0\} \to \widetilde{\beta}^0, \{\vartheta_\kappa'^0\}; \qquad \vartheta_{2n}'^0 = \vartheta_{2n}^0, \qquad \vartheta_{2n+1}'^0 = \pi - \vartheta_{2n+1}^0, \tag{21}$$

where n is an integer.

Now we assume that the potential energy has the form

$$V(\widetilde{\beta},\{\vartheta_\kappa\}) = V_\beta(\widetilde{\beta}) + \widetilde{\beta}^{-2}V_\vartheta(\{\vartheta_\kappa\}), \tag{22}$$

which enables us to factorize the wave function:

$$\psi_I^\pm(\widetilde{\beta},\{\vartheta_\kappa\}) = \widetilde{\beta}^{1-N/2}\phi_I^\pm(\widetilde{\beta})\chi^\pm(\{\vartheta_\kappa\}). \tag{23}$$

A real potential $V(\widetilde{\beta},\{\vartheta_\kappa\})$ may be a much more complicated function, but such a representation greatly simplifies further calculations. A similar function $V(\beta,\gamma)$ is adopted in a generalized description of nuclei which have only quadrupole deformation, given in §14 of Ref. [46]. Davydov's potential $V(\beta,\gamma)$ coincides with (22), when $\beta \to \widetilde{\beta}$ and $\gamma \to \{\vartheta_\kappa\}$.

The function $\chi^\pm(\{\vartheta_\kappa\})$ obeys the equation

$$\left[-\frac{\hbar^2}{2B}\Delta_\vartheta + \frac{\hbar^2 I(I+1)}{6B\mathcal{F}(\{\vartheta_\kappa\})} + V_\vartheta(\{\vartheta_\kappa\}) - \mathcal{E}_{I\nu}^\pm\right]\chi_\nu^\pm(\{\vartheta_\kappa\}) = 0. \tag{24}$$

Here the potential energy V_ϑ can be expanded in terms of displacements from one equilibrium position $(\vartheta_\kappa - \vartheta_\kappa^0)$ or another $(\vartheta_\kappa - \vartheta_\kappa'^0)$. The smallness of these displacements allows us to replace in (24) the function $\mathcal{F}(\{\vartheta_\kappa\})$ by its equilibrium value $\mathcal{F}_0 = \mathcal{F}(\{\vartheta_\kappa^0\})$ and the trigonometric functions $\sin\vartheta_\kappa$ or $\cos\vartheta_\kappa$ by $\sin\vartheta_\kappa^0$ or $\cos\vartheta_\kappa^0$ in the kinetic-energy operator. It can be easily shown that the relative error then is of the order $\sqrt{\overline{(\vartheta-\vartheta_0)^2}} \ll 1$, where the overbar means the quantum-mechanical average. As is usually done in molecular and solid-state physics [53], the following step will be the introduction of normal coordinates instead of $\vartheta - \vartheta_0$, which assures splitting of Eq. (24) into $N-2$ uncoupled oscillator equations with vibration frequencies $\omega_\nu^{(i)}$. Then the energy

$$\begin{aligned}\mathcal{E}_{I\nu}^\pm &= \mathcal{E}_\nu^\pm + \frac{\hbar^2 I(I+1)}{6B\mathcal{F}_0},\\ \mathcal{E}_\nu^\pm &= \sum_{i=1}^{N-2}\hbar\omega_\nu^{(i)}\left(\nu_i+\tfrac{1}{2}\right) \mp \tfrac{1}{2}\Delta\mathcal{E}_\nu,\end{aligned} \tag{25}$$

where the "angular" phonon numbers $\nu_i = 0, 1, 2, 3, \ldots$; $\nu = \{\nu_i\}$, $\Delta\mathcal{E}_\nu$ is the splitting of the νth level. Here $\mathcal{E}_\nu^+$ and $\mathcal{E}_\nu^-$ are yet doubly degenerate. Taking into account the tunneling under the potential barrier separated nuclear reflection-symmetry shapes leads to their splitting. Always $\mathcal{E}_\nu^+ < \mathcal{E}_\nu^-$ [52]. The functions $\chi_\nu^+(\{\vartheta_\kappa\})$ and $\chi_\nu^-(\{\vartheta_\kappa\})$ are, respectively, symmetric and antisymmetric combinations of the products of wave functions for uncoupled oscillators. We are not interested in their exact form.

Then for the function $\phi_I^\pm(\widetilde{\beta})$ one has the following equation:

$$\left[-\frac{\hbar^2}{2B}\frac{\partial^2}{\partial\widetilde{\beta}^2} + W_{I\nu}^\pm(\widetilde{\beta}) - E_{I\nu}^\pm\right]\phi_I^\pm(\widetilde{\beta}) = 0 \tag{26}$$

with the effective potential energy

$$W^{\pm}_{Iv}(\widetilde{\beta}) = W^{\pm}_{00}(\widetilde{\beta}) + \frac{\hbar^2 I(I+1)}{6B\mathcal{F}_0\widetilde{\beta}^2} + \frac{\mathcal{E}^{\pm}_{\nu} - \mathcal{E}_0}{\widetilde{\beta}^2}, \tag{27}$$

where $\mathcal{E}_0 = (\mathcal{E}^{+}_0 + \frac{1}{2}\mathcal{E}^{-}_0)$ and

$$W^{\pm}_{00}(\widetilde{\beta}) = V_{\beta}(\widetilde{\beta}) + \frac{(N-2)(N-4)\hbar^2}{8B\widetilde{\beta}^2} + \frac{\mathcal{E}_0}{\widetilde{\beta}^2}. \tag{28}$$

Choosing the potential energy $W^{\pm}_{00}(\widetilde{\beta})$) in the form

$$W^{\pm}_{00}(\widetilde{\beta}) = \frac{C}{2}\left(\frac{\widetilde{\beta}^2_0}{\widetilde{\beta}} - \widetilde{\beta}\right)^2, \tag{29}$$

this function $W(\widetilde{\beta})$ is only alternative to the parabolic curve taken in the original version of the Davydov–Chaban model. Since the amplitude of the nuclear vibrations is small, we can come to the harmonic approximation expanding the function (29) in powers of $\widetilde{\beta} - \widetilde{\beta}^0$. Then introducing the notations

$$\rho = \frac{\widetilde{\beta}}{\widetilde{\beta}_{00}}, \qquad \widetilde{\beta}^2_{00} = \frac{\hbar}{\sqrt{BC}}, \qquad \mu = \frac{\widetilde{\beta}_{00}}{\widetilde{\beta}_0},$$
$$E^{\pm}_{Iv} = \hbar\omega(\mathcal{K}^{\pm}_{Iv} - \mu^{-2}), \qquad \omega = (C/B)^{1/2}, \tag{30}$$

we transform (26) to

$$\left[-\frac{\partial^2}{\partial\rho^2} + \frac{A^{\pm}_{Iv}}{\rho^2} + \rho^2 - 2\mathcal{K}^{\pm}_{Iv}\right]\phi^{\pm}_{Iv}(\widetilde{\beta}) = 0, \tag{31}$$

where

$$A^{\pm}_{Iv} = \Delta^{\pm}_{\nu} + \frac{I(I+1)}{3\mathcal{F}_0}, \tag{32}$$

and

$$\Delta^{\pm}_{\nu} = \frac{1}{\mu^4} + \frac{2(\mathcal{E}^{\pm}_{\nu} - \mathcal{E}_0)}{\hbar\omega\widetilde{\beta}^2_{00}}. \tag{33}$$

Note, that $\Delta^{-} > \Delta^{+}$ and the sum $\Delta^{+}_{\nu} + \Delta^{-}_{\nu} = 2\mu^{-4}$ is always positive since the softness coefficient $\mu > 0$.

The solution of Eq. (31), which satisfies the normalization condition

$$\int_0^{\infty} (\phi^{\pm}_{Iv}(\widetilde{\beta}))^2 \,\mathrm{d}\widetilde{\beta} = 1 \tag{34}$$

and the boundary conditions $\phi(0) = \phi(\infty) = 0$, is given by

$$\phi^{\pm}_{nIv}(\widetilde{\beta}) = \sqrt{\frac{2\Gamma(n+1)}{\widetilde{\beta}_{00}\Gamma(n + s^{\pm}(Iv) + \frac{1}{2})}}\,\rho^{s^{\pm}(Iv)}\exp\left(-\tfrac{1}{2}\rho^2\right)\mathcal{L}^{s^{\pm}(Iv)-1/2}_n(\rho^2), \tag{35}$$

where $\Gamma(z)$ is the gamma function, $\mathcal{L}_n^{\alpha}(x)$ is the Laguerre polynomial, $n = 0, 1, 2, 3, \ldots$ and

$$s^{\pm}(I\nu) = \tfrac{1}{2}\left[1 + \sqrt{1 + 4A^{\pm}(I\nu)}\right]. \tag{36}$$

For energies one gets the expression

$$E^{\pm}_{nI\nu} = \hbar\omega(2n + \tfrac{1}{2} + s^{\pm}(I\nu) - \mu^{-2}). \tag{37}$$

Taking the energy of the ground state of the nucleus to be zero, one has

$$E^{\pm *}_{nI\nu} = E^{\pm}_{nI\nu} - E^{+}_{000} = \hbar\omega\left[2n + \frac{1}{2}\sqrt{1 + 4\Delta^{\pm}_{\nu} + \frac{4I(I+1)}{3\mathcal{F}_0}} - \frac{1}{2}\sqrt{1 + 4\Delta^{+}_{0}}\right]. \tag{38}$$

So, there are rotational bands, built on the vibrational states with a different number of "radial" phonons n and "angular" phonons $\nu = \{\nu_1, \nu_2, \nu_3, \ldots, \nu_{N-2}\}$. The parameters $\Delta^{\pm}_{\nu}$ depend only on ν, but not on n. For the main rotational bands of positive parity with sequence of spins $I^{\pi} = 0^+, 2^+, 4^+, \ldots$ and of negative parity with $I^{\pi} = 1^-, 3^-, 5^-, \ldots$ the quantum numbers $n = \nu = 0$. Strictly speaking, they are vibrational–rotational bands, since when the softness parameter $\mu \neq 0$, the vibrational wave function $\phi(\widetilde{\beta})$ essentially depends upon the rotation, i.e. on spin I (see also Ref. [46]). For $n \neq 0$ in (38) we need four fitting parameters ω, $\Delta^{\pm}$ and $\mathcal{F}_0$. But for the bands with $n = 0$ the situation simplifies by renormalization of frequency:

$$\omega \to \widetilde{\omega} = \frac{1}{\sqrt{3\mathcal{F}_0}}\omega. \tag{39}$$

Making use also of the new notation

$$d^{\pm}_{\nu} = \tfrac{3}{4}\mathcal{F}_0(1 + 4\Delta^{\pm}_{\nu}), \tag{40}$$

we rewrite Eq. (38) for $n = 0$ as

$$E^{\pm *}_{0I\nu} = \hbar\widetilde{\omega}\left[\sqrt{d^{\pm}_{\nu} + I(I+1)} - \sqrt{d^{+}_{0}}\right]. \tag{41}$$

So, here we have only three fitting parameters $\widetilde{\omega}$ and $d^{\pm}_{\nu}$ for both vibrational–rotational bands in analogy with our previous works [13–16].

3. Energy levels of odd nuclei

An odd nucleus can be treated as an even–even core plus an unpaired nucleon [15,44,46]. We again demand the rigid axial symmetry of the nucleus and direct axis ζ along the symmetry axis. The hamiltonian of such an odd nucleus is given by

$$\widehat{H} = -\sum_{\lambda=2}^{N}\frac{\hbar^2}{2B_\lambda}\frac{1}{\beta_\lambda^3}\frac{\partial}{\partial\beta_\lambda}\beta_\lambda^3\frac{\partial}{\partial\beta_\lambda} + \frac{\hbar^2(\widehat{I}^2 - \widehat{I}_\zeta^2)}{\sum_{\lambda=2}^{N}\lambda(\lambda+1)B_\lambda\beta_\lambda^2} + \widehat{H}_{\mathrm{Cor}} + V_0(\{\beta_\lambda\}), \tag{42}$$

where the operator $\widehat{H}_{\rm Cor}$ defines the Coriolis interaction of the unpaired nucleon with nuclear rotation:

$$\widehat{H}_{\rm Cor} = -\frac{\hbar^2(\widehat{I}_+\widehat{j}_- + \widehat{I}_-\widehat{j}_+)}{\sum_{\lambda=2}^{N}\lambda(\lambda+1)B_\lambda\beta_\lambda^2}. \tag{43}$$

Here $\widehat{I}$ and $\widehat{j}$ are, respectively, the nuclear and unpaired nucleon spin operators in units of $\hbar$,

$$\widehat{I}_\pm = \widehat{I}_\xi \pm i\widehat{I}_\eta, \qquad \widehat{j}_\pm = \widehat{j}_\xi \pm i\widehat{j}_\eta. \tag{44}$$

The solution of the Schrödinger equation (5) with this hamiltonian has the form

$$\Psi_I^\pm(\{\beta_\lambda\},\theta) = (\beta_2\beta_3\cdots\beta_N)^{-3/2}\psi_I^\pm(\{\beta_\kappa\})|IMKK\pm\rangle. \tag{45}$$

The functions $|IMKK\pm\rangle$, which describe now the rotation of the nucleus with spin projection K on the symmetry axis ζ, are given by [44]

$$|IMKK\pm\rangle = \sqrt{\frac{2I+1}{16\pi^2}}\left(D^I_{KM}(\theta)\varphi_K \pm (-1)^{I+K}D^I_{-KM}(\theta)\varphi_{-K}\right), \tag{46}$$

where the wave function φ_K describes the unpaired nucleon with the angular momentum projection K on the symmetry axis ζ. The total nuclear spin takes the values $I = K$, $K+1$, $K+2$, ... for levels of both parities. We assume that φ_K is not affected by the rotation.

The functions $\psi^\pm(\{\beta_\lambda\})$ describe the vibration of the even–even core. For transitions between two mirror nuclear shapes, i.e. as $\beta_\lambda \to (-1)^\lambda\beta_\lambda$, this function $\psi^\pm(\{\beta_\lambda\}) \to \pm\psi^\pm(\{(-1)^\lambda\beta_\lambda\})$. The functions $\psi^\pm(\{\beta_\lambda\})$ describe the even–even core of positive (ψ^+) or negative (ψ^-) parity. Then the complete parity of the nucleus π equals the product of this core parity and the parity of an unpaired nucleon state φ_K. Therefore, the superscript + or − of ψ stands only for the core parity and may differ from the parity π of the odd nucleus. Due to splitting always $E^+_{nI\nu} < E^-_{nI\nu}$, but the parity of the ground rotational band of odd nuclei can be both positive and negative.

For the functions $\psi_I^\pm(\{\beta_\lambda\})$ we again obtain Eqs. (12), (18) with $I(I+1)$ replaced by

$$f(I,K,\pm) = I(I+1) - K^2 \pm a(-1)^{I+1/2}(I+\tfrac{1}{2})\delta(K,\tfrac{1}{2}), \tag{47}$$

where $a = \langle\varphi_K|\widehat{j}_+|\varphi_{-K}\rangle$ is the decoupling parameter, $\delta(K,K') = 1$ for $K = K'$ and $\delta(K,K') = 0$ for $K \neq K'$.

Using spherical coordinates (15) and the potential energy (22), we again come to the same formulae (23)–(37) for the wave functions and energies, where $f(I,K,\pm)$ is substituted for $I(I+1)$. The energies of excited states relative to the ground-state energy with phonon numbers $n = \nu = 0$, spin K and parity π_0 are now:

$$E^{\pm *}_{nI^{\pi}\nu} = E^{\pm}_{nI^{\pi}\nu} - E^{+}_{0K^{\pi_0}0}$$

$$= \hbar\omega \left[2n + \tfrac{1}{2}\sqrt{1 + 4\Delta_\nu^{\pm} + \frac{4f(I,K,\pm)}{3\mathcal{F}_0}} - \tfrac{1}{2}\sqrt{1 + 4\Delta_0^{+} + \frac{4f(K,K,+)}{3\mathcal{F}_0}} \right]. \tag{48}$$

For the bands with phonon number $n = 0$ this expression simplifies:

$$E_{0I\pi_\nu}^{\pm *} = \hbar\widetilde{\omega} \left[\sqrt{d_\nu^{\pm} + f(I,K,\pm)} - \sqrt{d_0^{+} + f(K,K,+)} \right]. \tag{49}$$

4. Limiting cases

It is useful to consider the limiting case of a rigid rotator ($\mu = 0$). When $\mu \to 0$, the frequency $\omega \to \infty$, but their product remains constant:

$$\hbar\omega\mu^2 = \hbar\sqrt{\frac{C}{B}}\frac{\hbar}{\sqrt{BC}}\frac{1}{\widetilde{\beta}_0^2} = \frac{\hbar^2}{B\widetilde{\beta}_0^2}. \tag{50}$$

Then Eq. (41) for even–even nuclei transforms to

$$E_{0I0}^{+*} = AI(I+1), \tag{51}$$

$$E_{0I0}^{-*} = AI(I+1) + \Delta E, \tag{52}$$

where the rotor constant

$$A = \frac{\hbar^2}{6B\mathcal{F}_0\widetilde{\beta}_0^2} = \frac{\hbar^2}{\sum_{\lambda=2}^{N}\lambda(\lambda+1)B_\lambda(\beta_\lambda^0)^2} \tag{53}$$

and the energy shift for the negative-parity rotational band

$$\Delta E = \frac{\mathcal{E}_0^{-} - \mathcal{E}_0^{+}}{\widetilde{\beta}_0^2}. \tag{54}$$

Here ΔE depends both on the splitting of energies $\mathcal{E}_0^{-} - \mathcal{E}_0^{+}$, which correspond to ϑ-motion, and on the total nuclear deformation $\widetilde{\beta}_0$. For the rigid odd nuclei in (51), (52) we must only replace $I(I+1)$ by $f(I,K,\mp)$. In the general case of $\mu > 0$ the spectrum $E_{0I0}^{\pm *}$ may essentially deviate from the oversimplified law (51), (52).

For very soft nuclei or high spins

$$E_{0I0}^{\pm *} \approx \hbar\widetilde{\omega}\left(\sqrt{I(I+1)} + \frac{d_0^{\pm}}{2\sqrt{I(I+1)}} - \sqrt{d_0^{\pm}} \right). \tag{55}$$

The energy of the rotational level for a soft nucleus with high spin is proportional to $\sqrt{I(I+1)}$ in contrast to $I(I+1)$ for the rigid one.

5. Electric dipole, quadrupole and octupole transitions in even–even and odd nuclei

The reduced probability of the electric transition of multipolarity L from the state with spin I_i to the state with spin I_f is given by the expression [44]

$$B(\mathrm{E}L, I_i \to I_f) = \frac{1}{2I_i+1} \sum_{M_i M_f \mu} \left| \langle \Psi^{\pm}_{I_f}(\{\beta_\lambda\}, \theta) | \mathcal{M}_\mu(\mathrm{E}L) | \Psi^{\pm}_{I_i}(\{\beta_\lambda\}, \theta) \rangle \right|^2. \quad (56)$$

The electric multipole operator has the form

$$\mathcal{M}_m(\mathrm{E}L) = e \sum_{i=1}^{Z} r_i^L Y_{Lm}(\theta_i, \phi_i), \quad (57)$$

where e is the electric charge of the proton and r_i, θ_i, ϕ_i are the spherical coordinates of the ith proton in the laboratory coordinate system.

For EL transitions of multipolarity L ($2 \leqslant L \leqslant N$) in an axially symmetric nucleus we have

$$\mathcal{M}_m(\mathrm{E}L) = \sqrt{\frac{2L+1}{16\pi}} Q_0(L) \frac{\beta_L}{\beta_L^0} D^L_{0m}(\theta), \quad (58)$$

where

$$Q_0(L) = \frac{3}{\sqrt{(2L+1)\pi}} Z e R_0^L \beta_L^0 \quad (59)$$

is the L-pole moment of the static nucleus.

The operator of electric dipole transitions is connected with the polarized electric dipole moment (PEDM) [8–12] D_0 by

$$\mathcal{M}_m(\mathrm{E}1) = \sqrt{\frac{3}{4\pi}} D_0 \frac{\sum_{\lambda=2}^{(N-1)} a_\lambda \beta_\lambda \beta_{\lambda+1}}{\sum_{\lambda=2}^{(N-1)} a_\lambda \beta_\lambda^0 \beta_{\lambda+1}^0} D^1_{0m}(\theta), \quad (60)$$

where

$$a_\lambda = \frac{12(\lambda-1)(\lambda+1)(8\lambda+9)}{5(2\lambda+1)^{3/2}(2\lambda+3)^{3/2}}. \quad (61)$$

The value of the PEDM depends on the rearrangement of protons relative to neutrons both in the volume and on the surface. When the proton and neutron distributions in the nucleus have the same angular dependence, the PEDM is [11]

$$D_0 = \frac{AZe^3}{32\pi} \left(\frac{1}{J} + \frac{15}{8QA^{1/3}} \right) \sum_{\lambda=2}^{(N-1)} a_\lambda \beta_\lambda^0 \beta_{\lambda+1}^0. \quad (62)$$

Here J and Q are, respectively, coefficients associated with the volume and surface symmetry energy of the nucleus. Detailed discussions of different approaches to the PEDM can be found in Ref. [12].

Using our notation, we rewrite the electric L-pole operators in the form

$$\mathcal{M}_m(\mathrm{E}L) = \sqrt{\frac{2L+1}{16\pi}} Q_0(L) \frac{\widetilde{\beta}}{\widetilde{\beta}_0} \mathcal{G}_L(\{\vartheta\}) D^L_{0m}(\theta), \qquad 2 \leqslant L \leqslant N, \tag{63}$$

and

$$\mathcal{M}_m(\mathrm{E1}) = \sqrt{\frac{3}{4\pi}} D_0 \frac{\widetilde{\beta}^2}{\widetilde{\beta}_0^2} \mathcal{G}_1(\{\vartheta\}) D^1_{0m}(\theta), \tag{64}$$

where

$$\mathcal{G}_\lambda(\{\vartheta\}) = \frac{\widetilde{\beta}_\lambda/\widetilde{\beta}}{\widetilde{\beta}^0_\lambda/\widetilde{\beta}^0}, \qquad \lambda \geqslant 2,$$

$$\mathcal{G}_1(\{\vartheta\}) = \frac{\sum_{\lambda=2}^{(N-1)} a_\lambda \widetilde{\beta}_\lambda \widetilde{\beta}_{\lambda+1}/\widetilde{\beta}^2}{\sum_{\lambda=2}^{(N-1)} a_\lambda \widetilde{\beta}^0_\lambda \widetilde{\beta}^0_{\lambda+1}/\left(\widetilde{\beta}^0\right)^2}. \tag{65}$$

Below we shall obtain an expression for the reduced probabilities of electric transitions in even–even nuclei. Calculating those in odd nuclei we can neglect the small contribution from the unpaired nucleon [15,46], then it leads to coincidence of the formulae for even–even and odd nuclei.

For the reduced probabilities of EL transitions between levels $|n_\mathrm{i} I_\mathrm{i} 0\rangle$ and $|n_\mathrm{i} I_\mathrm{f} 0\rangle$, using functions (6), (7), (23) and (35), we find the expressions

$$B(\mathrm{E}L, I_\mathrm{i} \to I_\mathrm{f}) = B_\mathrm{a}(\mathrm{E}L, I_\mathrm{i} \to I_\mathrm{f}) S^2(\mathrm{E}L, I_\mathrm{i} \to I_\mathrm{f}) \mathcal{G}_L. \tag{66}$$

Here

$$B_\mathrm{a}(\mathrm{E}L, I_\mathrm{i} \to I_\mathrm{f}) = \frac{2L+1}{16\pi} Q_0^2(L) \langle I_\mathrm{i} L 00 | I_\mathrm{f} 0\rangle^2, \qquad 2 \leqslant L \leqslant N, \tag{67}$$

$$B_\mathrm{a}(\mathrm{E1}, I_\mathrm{i} \to I_\mathrm{f}) = \frac{3}{4\pi} D_0^2 \langle I_\mathrm{i} 100 | I_\mathrm{f} 0\rangle^2, \qquad L = 1 \tag{68}$$

are the reduced probabilities of EL transitions in the rigid axially symmetric rotor, and the factors

$$S(\mathrm{E}L, I_\mathrm{i} \to I_\mathrm{f}) = \int_0^\infty \mathrm{d}\widetilde{\beta}\, \phi^\pm_{n_\mathrm{i} I_\mathrm{i} 0}(\widetilde{\beta}) \frac{\widetilde{\beta}}{\widetilde{\beta}^0} \phi^\pm_{n_\mathrm{f} I_\mathrm{f} 0}(\widetilde{\beta}), \qquad 2 \leqslant L \leqslant N, \tag{69}$$

$$S(\mathrm{E1}, I_\mathrm{i} \to I_\mathrm{f}) = \int_0^\infty \mathrm{d}\widetilde{\beta}\, \phi_{n_\mathrm{i} I_\mathrm{i} 0}(\widetilde{\beta}) \left(\frac{\widetilde{\beta}}{\widetilde{\beta}^0}\right)^2 \phi_{n_\mathrm{f} I_\mathrm{f} 0}(\widetilde{\beta}) \tag{70}$$

are due to deformational $\widetilde{\beta}$ oscillations of the nucleus (see also Refs. [14-16,44,45,55]);

$$\mathcal{G}_L = \int \mathrm{d}\Omega\, \chi_0(\{\vartheta_\kappa\}) \mathcal{G}_L(\{\vartheta\}) \chi_0(\{\vartheta_\kappa\}), \tag{71}$$

$\langle I_\mathrm{i} L 00 | I_\mathrm{f} 0\rangle$ is a Clebsch–Gordan coefficient.

In the case of transitions between levels $|nI_i0\rangle$ and $|0I_f0\rangle$ the factor $S(EL, I_i \to I_f)$ is (see also Refs. [14-16,44,45,55])

$$S(EL, I_i \to I_f) = \mu \frac{\Gamma\left(1+\frac{1}{2}(s_i+s_f)\right)\Gamma\left(n+\frac{1}{2}(s_i-s_f-1)\right)}{\sqrt{n!\Gamma\left(s_f+\frac{1}{2}\right)\Gamma\left(n+s_i+\frac{1}{2}\right)\Gamma\left(\frac{1}{2}(s_i-s_f-1)\right)}}, \quad L \geqslant 2, \tag{72}$$

$$S(E1, I_i \to I_f) = \mu^2 \frac{\Gamma\left(\frac{3}{2}+\frac{1}{2}(s_i+s_f)\right)\Gamma\left(n+\frac{1}{2}(s_i-s_f-1)-1\right)}{\sqrt{n!\Gamma\left(s_f+\frac{1}{2}\right)\Gamma\left(n+s_i+\frac{1}{2}\right)\Gamma\left(\frac{1}{2}(s_i-s_f)-1\right)}}, \tag{73}$$

where $\Gamma(x)$ is the gamma function, $s_i = s(I_i0)$ and $s_f = s(I_f0)$. Here for the sake of simplicity we omit the parities of initial and final states.

While the reduced probabilities of transitions depend on the constant $\mathcal{G}_L$, the ratio

$$\begin{aligned} R(I,L) &= \frac{B(EL, I \to I+L)}{B(EL, 0 \to L)} \\ &= \frac{B_a(EL, I \to I+L)}{B_a(EL, 0 \to L)} \frac{S^2(EL, I \to I+L)}{S^2(EL, 0 \to L)} \\ &= \left(\frac{\langle IL00|(I+L)0\rangle}{\langle 0L00|L0\rangle} \frac{S(EL, I \to I+L)}{S(EL, 0 \to L)} \right)^2 \end{aligned} \tag{74}$$

does not contain it at all. This ratio has the factor

$$\frac{S(EL, I \to I+L)}{S(EL, 0 \to L)}$$

connected with stretching of the nucleus due to rotation.

Within the main bands ($n = \nu = 0$) there were measured also in a variety of nuclei [1,2,17-27,29-40] the branching ratios

$$W(I) = \frac{B(E1, I \to I-1)}{B(E2, I \to I-2)}, \tag{75}$$

for which one finds

$$\begin{aligned} W(I) &= W_a(I) \left(\frac{S(E1, I \to I-1)}{S(E2, I \to I-2)} \frac{\mathcal{G}_1}{\mathcal{G}_2} \right)^2 \\ &= \frac{8(2I-1)}{5(I-1)} \left(\frac{D_0}{Q_0(2)} \right)^2 \left(\frac{S(E1, I \to I-1)}{\mu S(E2, I \to I-2)} \mathcal{G}_{12} \right)^2. \end{aligned} \tag{76}$$

This ratio depends upon an additional parameter $\mathcal{G}_{12} = \mu\mathcal{G}_1/\mathcal{G}_2$. The absolute values of the parameter $\mathcal{G}_{12}$ can be between 0 and 1, see also Refs. [14,15].

Table 1
Fitting parameters of even–even nuclei. N indicates the number of the figure containing the level scheme for these nuclei

N	Nucleus	$\hbar\widetilde{\omega}$ [keV]	d_0^+	d_0^-
1	^{144}Ba	275.7	17.58	36.67
2	^{146}Ba	240.4	9.516	28.63
3	^{146}Ce	259.3	4.955	17.33
4	^{146}Nd	322.2	1.339	6.640
5	^{148}Nd	263.1	3.165	13.87
6	^{150}Nd	312.5	65.76	110.3
7	^{150}Sm	319.0	12.13	26.23
8	^{220}Rn	118.8	0.053	26.41
9	^{222}Rn	113.0	0.562	32.02
10	^{218}Ra	203.9	0.889	5.561
11	^{220}Ra	198.1	20.84	22.63
12	^{222}Ra	94.01	2.854	15.20
13	^{224}Ra	182.8	46.70	56.08
14	^{226}Ra	210.3	101.1	115.3
15	^{228}Ra	133.4	29.71	78.25
16	^{220}Th	207.5	0.879	0.879
17	^{222}Th	241.0	42.50	50.05
18	^{224}Th	236.3	77.69	86.27
19	^{226}Th	249.6	129.3	141.4
20	^{228}Th	201.5	98.83	125.8

6. Comparison with experimental data

Applying Eqs. (41), (49) for numerical calculations of the energies, we use the fitting parameters d^+ and d^- for positive- and negative-parity main rotational bands, respectively. Furthermore, the parameter $\hbar\widetilde{\omega}$ is the same for both bands and the additional decoupling parameter a is used in the case of odd nuclei with $K = \frac{1}{2}$. We have been trying to reproduce the positions of all known experimental energies by means of the least-squares method. In this way the sum of absolute deviations between calculated and experimental energies for each level has been minimized in contrast to our previous works [13–16], where we looked for the minimum of the sum of relative deviations of these data. These numerical results are compared with experimental data for a number of even–even and odd isotopes of Ba, Ce, Nd, Pm, Sm, Rn, Fr, Ra, Ac and Th in Figs. 1–37. Here we analyze practically the full set of nuclei having equilibrium octupole deformation. In previous works [13–16] we considered only isotopes of Ra, Th and Ac and took into account only quadrupole and octupole deformations. Tables 1 and 2 contain the values of fitting parameters $\hbar\widetilde{\omega}$, $d^{\pm}$ and a for even–even and odd nuclei correspondingly. Note that such states really have a rotational nature, which is based on the following well-known facts. The states of the same parity are related by strong E2 transitions and those of the bands with opposite parity by E1 cross-band transitions.

Table 2
Fitting parameters of odd nuclei. N indicates the number of the figure containing the level scheme for these nuclei

N	Nucleus	$\hbar\widetilde{\omega}$ [keV]	d_0^+	d_0^-	a
21	^{151}Pm	268.2	99.82	103.0	–
22	^{217}Fr	217.1	21.12	21.42	–
23	^{219}Fr	194.4	912.0	975.6	9.24
24	^{221}Fr	70.39	34.16	54.41	4.41
25	^{219}Ra	254.0	82.78	85.86	2.37
26	^{221}Ra	89.60	25.66	39.01	–
27	^{223}Ra	271.4	526.7	536.0	–
28	^{225}Ra	140.8	138.9	143.6	1.6
29	^{227}Ra	30.71	3.349	22.92	–
30	^{219}Ac	198.4	5.913	6.891	0.5
31	^{223}Ac	230.9	425.6	438.6	–
32	^{225}Ac	57.07	14.06	19.76	–
33	^{227}Ac	74.30	26.42	27.02	–
34	^{221}Th	255.8	78.12	78.13	–
35	^{223}Th	315.1	364.1	368.7	–
36	^{225}Th	425.7	949.9	951.1	–
37	^{229}Th	259.8	444.3	532.5	–

All this led experimentators to a derivation of schemes for rotational bands, which have been used by us, see Figs. 1–37. Only for the isotope ^{219}Ra we treat two experimentally observed bands as a single one (this case to be discussed in Subsection 5.3). Note that the energy of some levels of rotational bands have not been determined in experiment for several isotopes. In these cases we predict the position of absent levels.

6.1. Energy-level schemes of middle even–even nuclei

First, we discuss even–even middle nuclei Ba, Ce, Nd, Sm, see Figs. 1–7. In these nuclei we can see two rotational bands of opposite parity. As a rule the first 2^+ states in these nuclei have the energy 200–300 keV and the energies of the 1^- states are near to 550 keV. The simple expression (41) describes well both rotational bands in all isotopes of Ba, Ce, Nd, Sm. Note that the largest number of levels is measured for ^{150}Sm [35] in this group of nuclei. The comparison of the experimental and theoretical levels for ^{150}Sm is presented in Fig. 7. We can see an excellent agreement of experimental and theoretical level energies of the positive-parity band. However, we should note the bad correlation of these data in the case of close 1^- and 3^- states provided by Figs. 1, 2, 6. This tendency takes place also for heavy even–even nuclei (see, for example, Figs. 8, 9, 18, 19). We are predicting the position of the 1^- states for the isotopes ^{146}Ce, ^{146}Nd, ^{148}Nd and ^{150}Sm, for which the corresponding experimental observations are still absent.

The fitting parameters $\hbar\widetilde{\omega}$ and $d_0^{\pm}$ have a small range of variation for isotopes of ^{144,146}Ba, ^{146}Ce, ^{146,148}Nd, ^{150}Sm (see Table 1). The fluctuations of the parameters $\hbar\widetilde{\omega}$

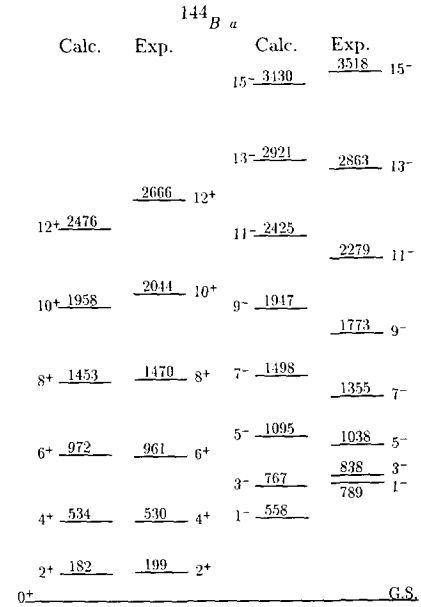

Fig. 1. Experimental [34] and calculated energy levels of ^{144}Ba in (keV). The position of 1^-.

and $d_0^{\pm}$ are connected with variation of deformation, momentum of inertia and shape softness in these isotopes. We stress here that the softness variation in these isotopes is small, because the parameters $d_0^{\pm}$ are proportional with μ^{-4}. In this case variation of the softness μ is many times smaller than variation of $d_0^{\pm}$ given in Table 1. Therefore, all these nuclei have close values of the shape softness.

The parameters $d_0^{\pm}$ for ^{150}Nd have larger values than in all other nuclei from this

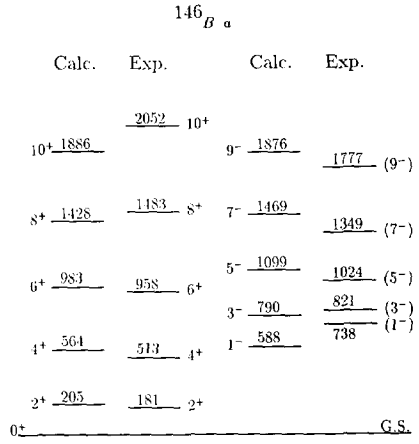

Fig. 2. Experimental [34] and calculated energy levels of ^{146}Ba in (keV).

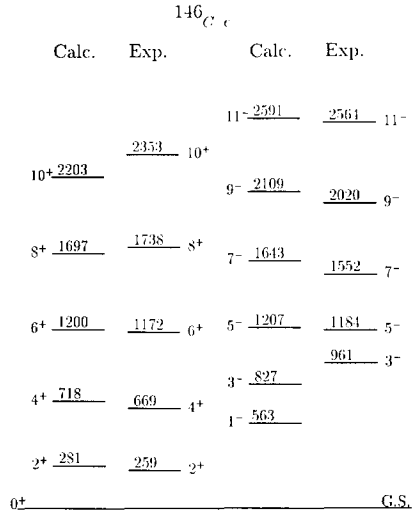

Fig. 3. Experimental [36] and calculated energy levels of ^{146}Ce in (keV). We are predicting the position of the 1^- state for ^{146}Ce, for which the corresponding experimental observation is absent [36].

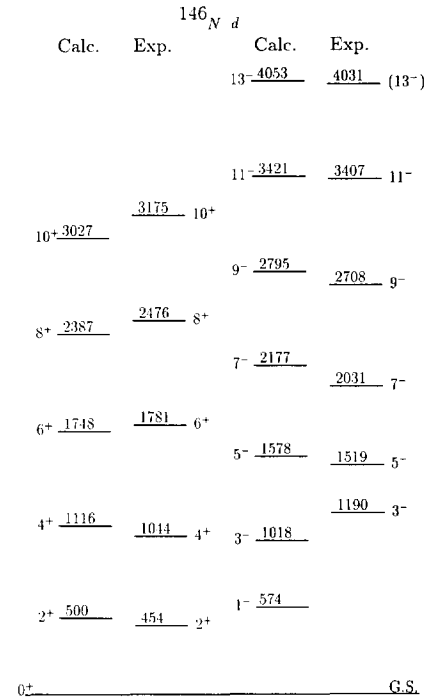

Fig. 4. Experimental [2] and calculated energy levels of ^{146}Nd in (keV). We are predicting the position of the 1^- state for ^{146}Nd, for which the corresponding experimental observation is absent [2].

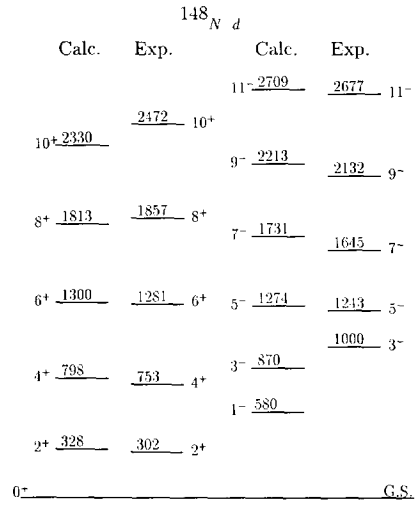

Fig. 5. Experimental [2] and calculated energy levels of ^{148}Nd in (keV). We are predicting the position of the 1^- state for ^{148}Nd, for which the corresponding experimental observation is absent [2].

group. Note that according to the calculation of Ref. [7] this nucleus has no equilibrium octupole deformation, but its level structure (see Fig. 6) and intensive dipole cross-band transitions support the point of view that ^{150}Nd has equilibrium octupole deformation. The agreement of calculated and experimental energies for ^{150}Nd presented in Fig. 6 is excellent for positive parity and is good for the band of negative parity. The agreement of these quantities for the band of negative parity in ^{150}Sm is also quite satisfactory.

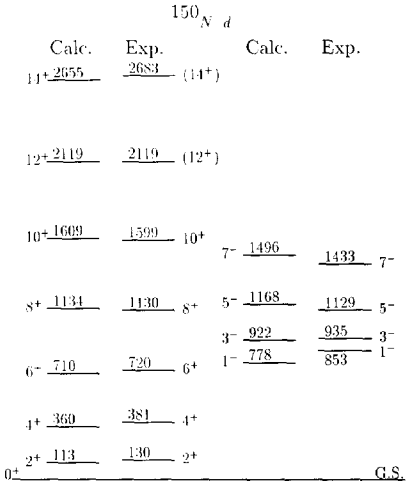

Fig. 6. Experimental [2] and calculated energy levels of ^{150}Nd in (keV).

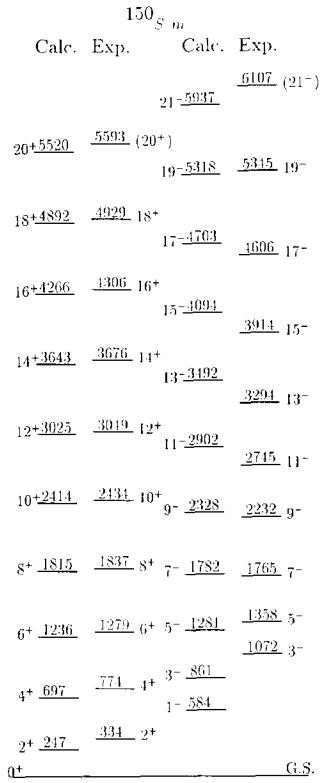

Fig. 7. Experimental [35] and calculated energy levels of ^{150}Sm in (keV). We are predicting the position of the 1^- state for ^{150}Sm, for which the corresponding experimental observation is absent [35].

6.2. *Energy-level schemes of heavy even–even nuclei*

A comparison of experimental and theoretical energy levels for heavy even–even nuclei is presented in Figs. 8–20. The isotope dependencies of level structure and fitting parameters can be analyzed for Ra and Th. The energy of the first 2^+ levels in isotopes of Rn, Ra and Th decreases with growing neutron number and has smaller value than for middle nuclei. The energies of the 1^- states in heavy nuclei are also lower than in

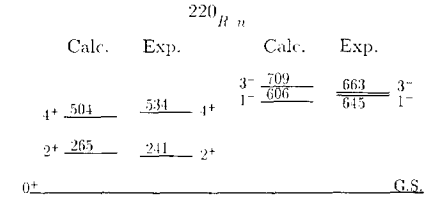

Fig. 8. Experimental [37] and calculated energy levels of ^{220}Rn in (keV).

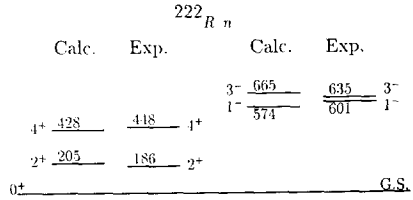

Fig. 9. Experimental [37] and calculated energy levels of ^{222}Rn in (keV).

middle nuclei. Unfortunately, the first states of the negative-parity band are not observed in all isotopes of Ra and Th. However, the dependence of energy of the 1^- states on neutron number is not monotonous in contrast to the case of the 2^+ states, see the discussion in Ref. [25]. The position of the 1^- state in even–even nuclei depends on the height and width of the potential barrier separating potential wells with opposite deformation parameters of odd multipolarity. We predict the position of the first states of negative-parity bands in many isotopes, which may be observed experimentally.

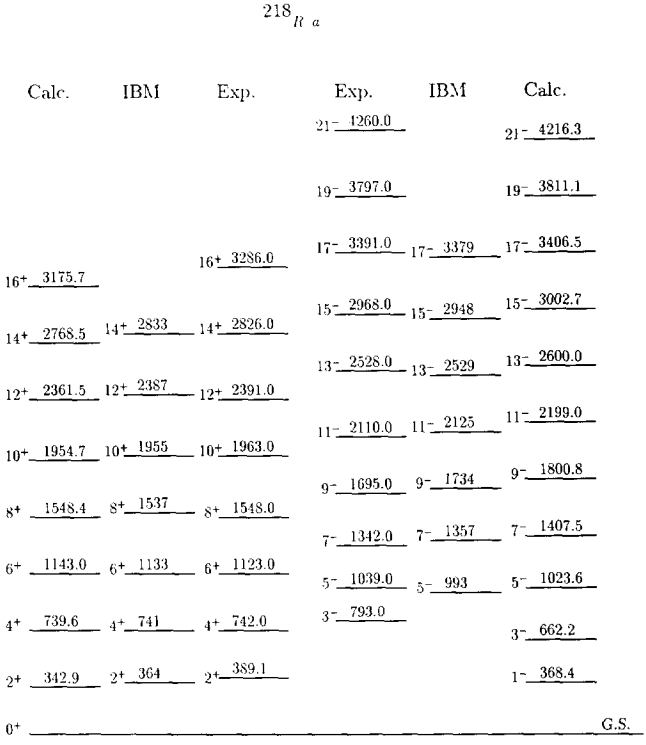

Fig. 10. Experimental [18,19] and theoretical energy levels of ^{218}Ra (in keV). Theoretical energy levels obtained in the framework of the interaction boson model (IBM) are taken from Ref. [18]. We are predicting the position of the 1^- state for ^{218}Ra, for which the corresponding experimental observation is absent [18,19,58].

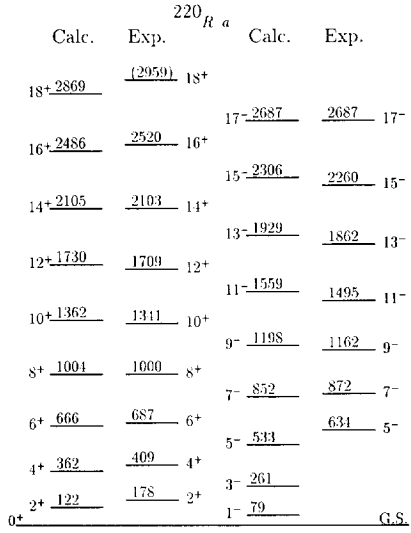

Fig. 11. Experimental [23] and calculated energy levels of ^{220}Ra in (keV). We are predicting the position of the 1^- and 3^- states for ^{220}Ra, for which the corresponding experimental observations are absent [23].

The parameter $\hbar\tilde{\omega}$ for these nuclei is smaller than for middle atomic-weight nuclei, see Table 1. This parameter has a small variation practically for all even–even heavy nuclei. The deviations from the average value of the parameter $\hbar\tilde{\omega}$ exist in isotopes ^{222,228}Ra. Note, that these two isotopes have a small number of known levels, that leads to a small accuracy of extraction of fitting parameters.

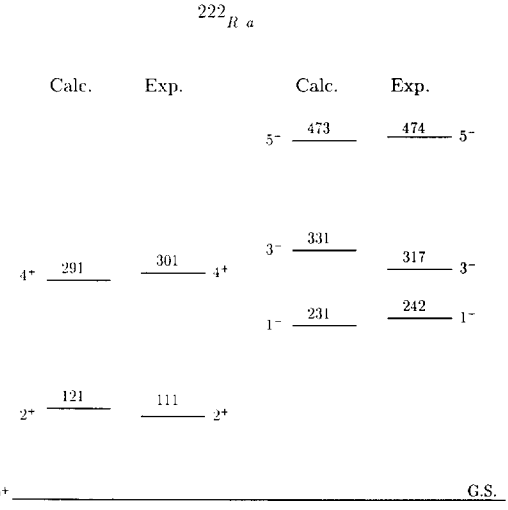

Fig. 12. Experimental [25] and calculated energy levels of ^{222}Ra in (keV).

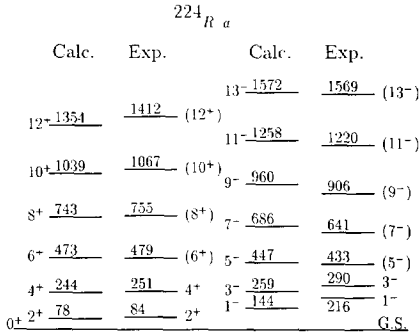

Fig. 13. Experimental [26] and calculated energy levels of ^{224}Ra in (keV).

The values of the parameters $d_0^{\pm}$ increase and, respectively, the softness parameter μ decreases with growing neutron number in even–even Th isotopes. The fitting parameters $d^{\pm}$ presented in Table 1 give rise to the conclusion that increasing the neutron number in the isotope chain of even–even nuclei seems to be connected with the transition from soft nuclei with respect to the shape deformation to the more rigid ones. The spectrum of more heavy isotopes is more close to the simple rotator spectrum. Finally, one can point out that the spectra of Ra and Th isotopes known to very high spins are satisfactorily described by the very simple formula (41), as follows from Figs. 10–12, 14, 16–20.

In Fig. 10 we compare also our calculations with the results of the interacting boson model (IBM) available [18] for ^{218}Ra. We see that our model has a sightly worse description than the IBM. However, the IBM uses four fitting parameters for even–even nuclei, whereas our model has only three ones.

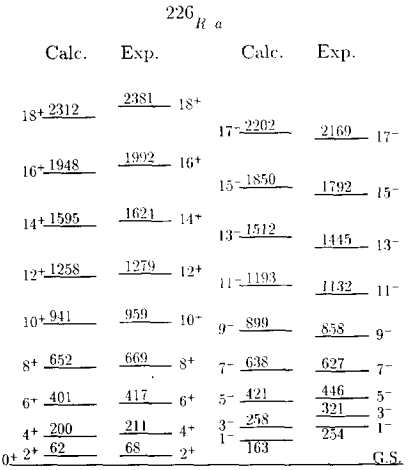

Fig. 14. Experimental [27] and calculated energy levels of ^{226}Ra in (keV).

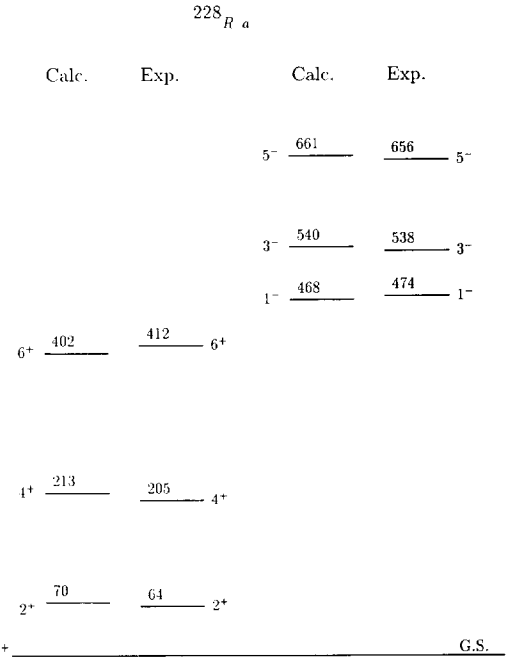

Fig. 15. Experimental [27] and calculated energy levels of ^{228}Ra in (keV).

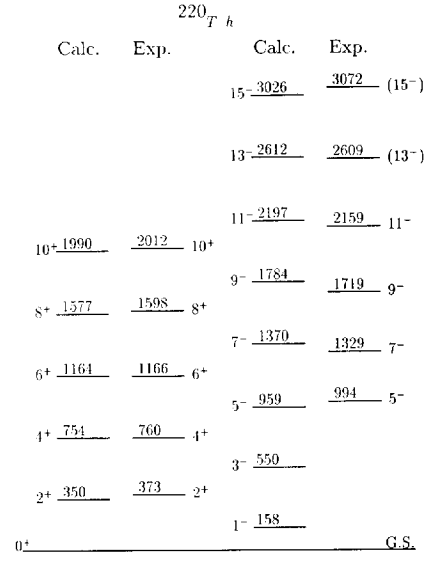

Fig. 16. Experimental [29] and calculated energy levels of ^{220}Th in (keV). We are predicting the position of the 1^- and 3^- states for ^{220}Th, for which the corresponding experimental observations are absent [29].

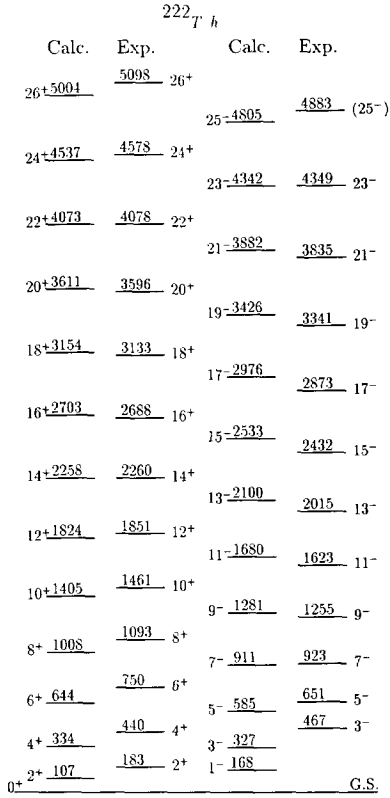

Fig. 17. Experimental [29] and calculated energy levels of ^{222}Th in (keV). We are predicting the position of the 1^- states for ^{220}Th, for which the corresponding experimental observation is absent [29].

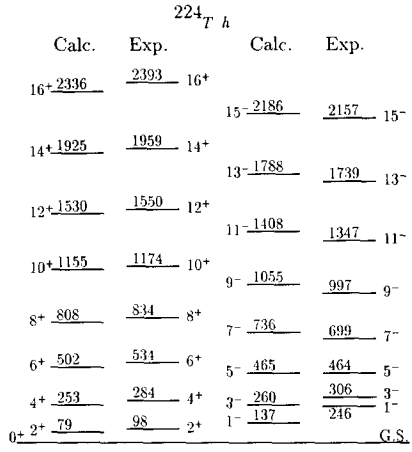

Fig. 18. Experimental [31] and calculated energy levels of ^{224}Th in (keV).

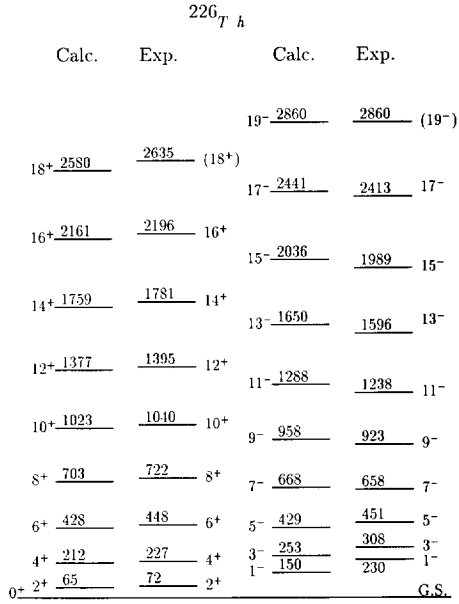

Fig. 19. Experimental [31] and calculated energy levels of ^{226}Th in (keV).

6.3. *Energy-level scheme of odd nuclei*

The comparison between experimental and theoretical data for the main rotational bands of odd nuclei is presented in Figs. 21–37.

The agreement between the experimental and theoretical level scheme for ^{151}Pm presented in Fig. 21 is good for both parity bands.

In heavy odd nuclei we can analyze the isotope dependencies of level structure and fitting parameters for Ra, Ac and Th. The energy level density in odd heavy isotopes is

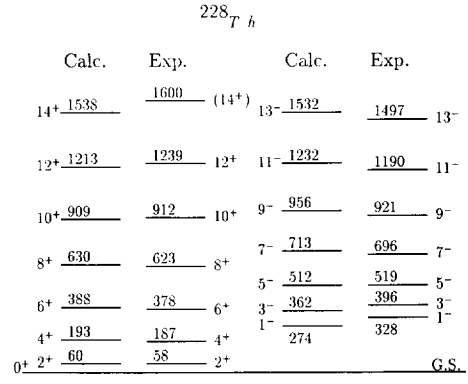

Fig. 20. Experimental [31] and calculated energy levels of ^{228}Th in (keV).

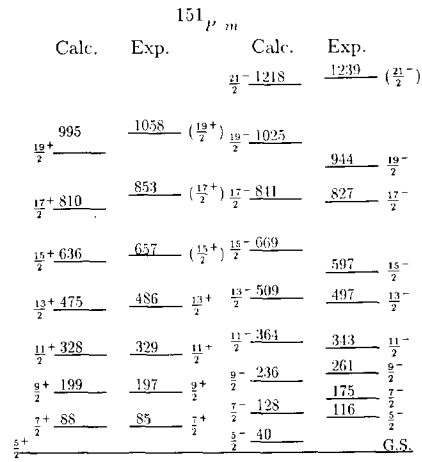

Fig. 21. Experimental [2] and calculated energy levels of ^{151}Pm in (keV).

larger than in even–even ones.

Note that sometimes the ground state of odd nuclei has negative parity, see, for example, Ac isotopes. For such nuclei the sign of the parameters $d^{\pm}$ associated with the reflection symmetry of the core, does not coincide with the parity of the nuclear bands.

The fitting parameters $\hbar\widetilde{\omega}$, $d_0^{\pm}$ and a for odd nuclei have larger variation than for even–even heavy nuclei, see Table 2. It is connected with a wide range of variation for the first excited-state energies of positive and negative parities. As a result there

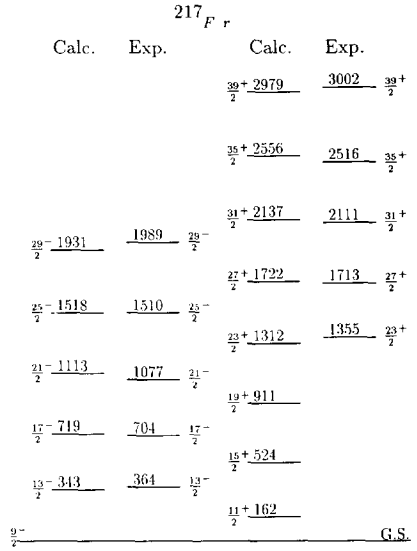

Fig. 22. Experimental [40] and calculated energy levels of ^{217}Fr in (keV). We are predicting the position of the $\frac{11}{2}^+$, $\frac{15}{2}^+$ and $\frac{19}{2}^+$ states for ^{217}Fr, for which the corresponding experimental observations are absent [40].

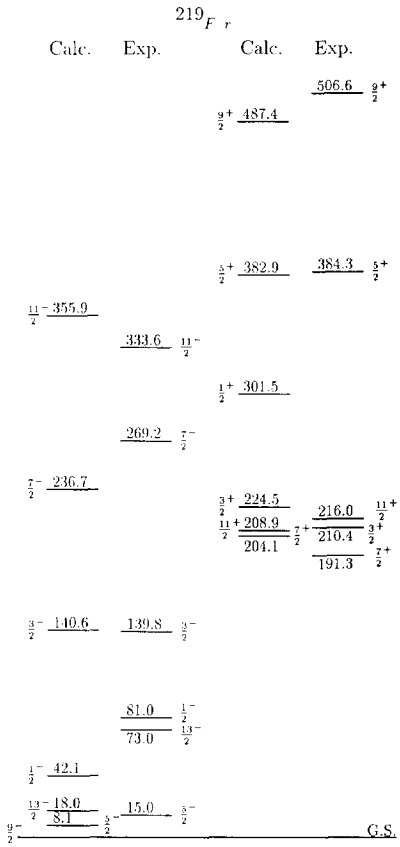

Fig. 23. Experimental [41] and calculated energy levels of ^{219}Fr in (keV). We are predicting the position of the $\frac{1}{2}^+$ state for ^{219}Fr, for which the corresponding experimental observation is absent [41].

is no simple monotonous dependence of the parameters $\hbar\widetilde{\omega}$ and $d_0^{\pm}$ on the number of neutrons. Here we point out that a small number of levels is measured in the main rotational bands of ^{223,225}Ra and ^{229}Th, therefore the fitting parameters for these nuclei are not extracted with desired accuracy and may change if additional levels will be measured.

The isotopes ^{221,223,225,227}Ra are more soft to shape deformation due to rotation than the nearest even–even ones (see Tables 1 and 2, where the parameters $d_0^{\pm}$ for odd isotopes are larger than for even–even isotopes of Ra). In contrast to this, the isotopes ^{223,225,229}Th are more rigid to shape deformation than the nearest even–even ones.

We pointed here that the spectrum of levels in several isotopes of Fr, Ra, Ac and Th is known up to very high values of spin and we satisfactorily describe them with the help of the very simple expression (49), see Figs. 22, 25, 27, 30, 33–36.

In Figs. 28–30, 32–34 we present also the results of the microscopic model by Leander and Chen [5]. We see that our model gives a better description than the microscopic model for isotopes ^{223,225,227}Ra, ^{223,225}Ac and sightly worse description for the isotope

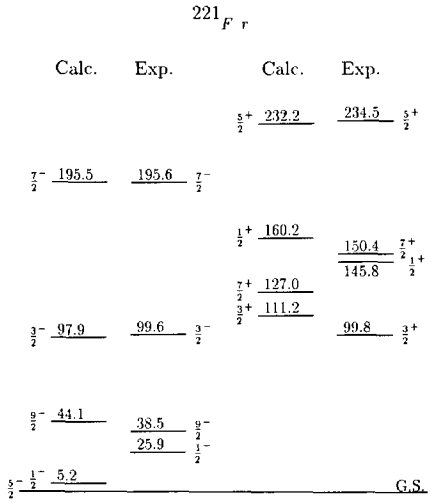

Fig. 24. Experimental [41] and calculated energy levels of ^{221}Fr in (keV).

^{227}Ac. The values of level energies of the odd-parity band for Ra isotopes calculated in the framework of the microscopic approach [5] are systematically higher than the corresponding experimental data and our calculations. Note that we consider here only the main rotational band in contrast to Ref. [5].

For nuclei of ^{219,221}Fr there is a microscopic calculation of Kvasil et al. [41], whose excellent description of experimental data is better than ours, see Figs. 23 and 24. However, we note that our model is much simpler and clearer than any microscopic model and is not connected with complicated calculations.

In all odd isotopes except ^{217}Fr, ^{219}Ra and ^{221}Th the rotational bands have spins $I_0^{\pm}$, $(I_0+1)^{\pm}$, $(I_0+2)^{\pm}$, $(I_0+3)^{\pm}$, $(I_0+4)^{\pm}$, ..., i.e. there realizes a strong coupling between the even–even core and unpaired nucleon, which we accepted in Section 3.

The situation with the level scheme in ^{217}Fr, ^{219}Ra and ^{221}Th nuclei is not clear up to now. The sequence of levels in these three nuclei is the same as in even–even nuclei, i.e. I_0^+, $(I_0+2)^+$, $(I_0+4)^+$, ... in positive-parity bands and $(I_0+1)^-$, $(I_0+3)^-$, $(I_0+5)^-$, ... in negative-parity bands [40,20,32]. These isotopes are theoretically considered [2,20] in the approximation of weak coupling between the even–even core and unpaired nucleon. In the limit of weak coupling between core and unpaired nucleon one can neglect a contribution of the unpaired nucleon and to obtain the expression for the level energy similar to (41). In this case the sequence of spins is the same as in even–even nuclei, see also Ref. [44]. However, recently a more complete scheme of ^{219}Ra is observed [22], which has two additional bands in comparison with Ref. [20]. Here we assume that the additional band marked I in Ref. [22] along with the bands, found previously [20], form usual bands with spins $I_0^{\pm}$, $(I_0+1)^{\pm}$, $(I_0+2)^{\pm}$, ... Since ^{219}Ra has $K=\frac{1}{2}$, the sequence of spins can be permutated. The comparison of such an experimental scheme of levels with our theoretical calculation is presented in Fig. 25.

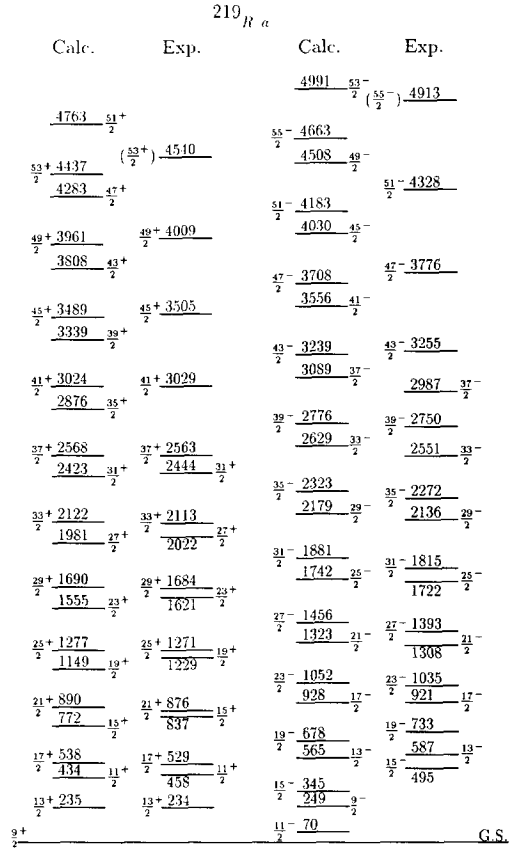

Fig. 25. Experimental [20,22] and calculated energy levels of ^{219}Ra in (keV). We are predicting the position of the $\frac{9}{2}^-$, $\frac{11}{2}^-$, $\frac{35}{2}^+$, $\frac{39}{2}^+$, $\frac{41}{2}^-$, $\frac{43}{2}^+$, $\frac{45}{2}^-$, $\frac{47}{2}^+$, $\frac{49}{2}^-$, $\frac{51}{2}^+$, $\frac{53}{2}^-$ and $\frac{53}{2}^+$ states for ^{219}Ra, for which the corresponding experimental observations are absent [20,22].

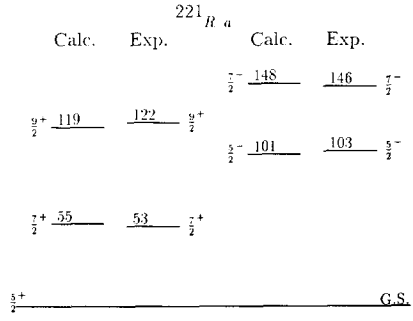

Fig. 26. Experimental [24] and calculated energy levels of ^{221}Ra in (keV).

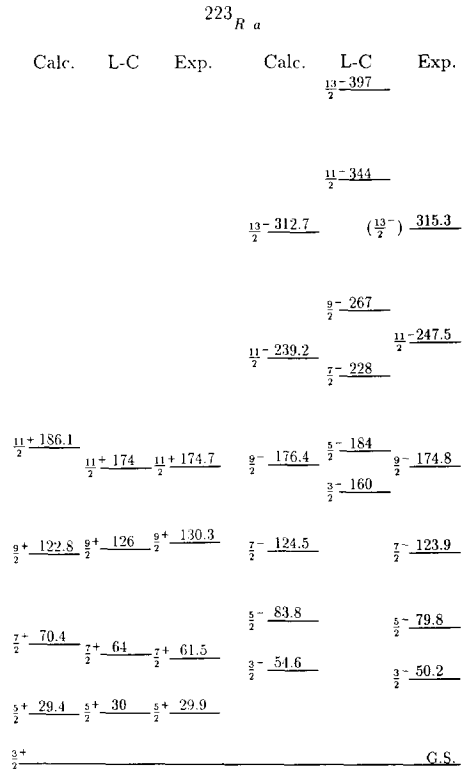

Fig. 27. Experimental [2] and calculated energy levels of ^{223}Ra in (keV). The theoretical energy levels obtained in the framework of the microscopic model by Leander and Chen (L–C) are taken from Ref. [5].

Following Refs. [2,20], we assume that the ground state of ^{219}Ra has spin $\frac{9}{2}^+$. This value of spin of the ground state is not completely rejected in Ref. [21], where the spin of the ground state is determined from α-decay of ^{223}Th. Note that the determination of the level spin from α-decay is not unique, see also the discussion in Ref. [21]. We can see the excellent agreement between theoretical and experimental data in Fig. 25. If we make the assumption that the ground-state spin is $\frac{7}{2}^+$, then χ^2 deviations between calculated and experimental values of level energies is greater in comparison with our result for $I_{\mathrm{G.S.}} = \frac{9}{2}^+$. It would be useful to remeasure the spectra of ^{217}Fr and ^{221}Th with higher accuracy. These nuclei have also $K = \frac{1}{2}$, therefore the situation with side bands and type of coupling is not quite clear. The results for ^{217}Fr and ^{221}Th in the weak-coupling approximation are presented in Figs. 22 and 34 correspondingly.

Comparing the experimental and theoretical values of the level energies in Figs. 1–37 we can conclude that the very simple expressions (41) and (49) give a good description.

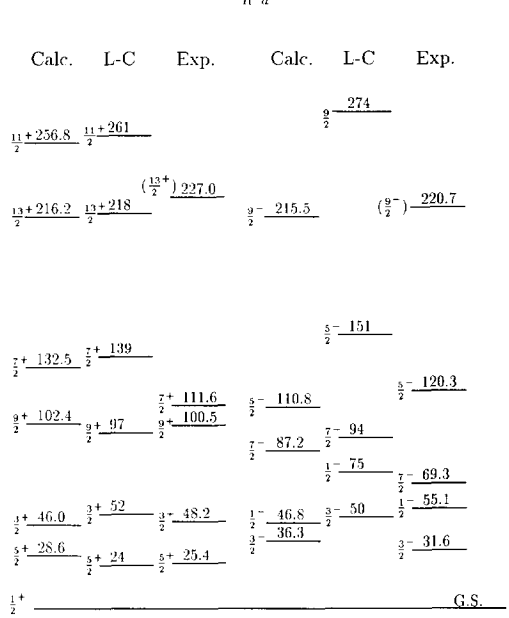

Fig. 28. Experimental [2] and calculated energy levels of ^{225}Ra in (keV). The theoretical energy levels obtained in the framework of the microscopic model by Leander and Chen (L–C) are taken from Ref. [5].

6.4. *Transition probability*

The experimental information about transition probabilities is not so rich as for energy levels. Nevertheless there are some measurements to be analyzed below.

Now we shall be engaged with the different ratios of transition probabilities between levels of the main bands. The ratio of reduced probabilities depends on the parameter $s^{\pm}(I,0)$, which is related to the parameters $\Delta^{\pm}$ (see Eqs. (32), (33), (36)). They may be easily expressed in terms of the parameters $d^{\pm}$:

$$s^{\pm}(I0) = \frac{1}{2}\left[1 + \frac{2}{\sqrt{3\mathcal{F}_0}}\sqrt{d^{\pm} + I(I+1)}\right], \tag{77}$$

where the factor $I(I+1)$ is replaced by $f(I,K,\pm)$ for odd nuclei.

For numerical calculations of the transition probabilities ratios we employ the parameters $d^{\pm}$ from Tables 1 and 2, which are already found during the fitting of energy levels. There remains the uncertain parameter $\mathcal{F}_0$. It may be estimated, taking the hydrodynamics ratios of the mass parameters B_λ and $B_{\lambda+1}$ [44]

$$\frac{B_{\lambda+1}}{B_\lambda} = \frac{\lambda}{\lambda+1} \tag{78}$$

and equilibrium deformation parameters β_λ^0, calculated in Ref. [7] by the shell-correction method [57]. Then

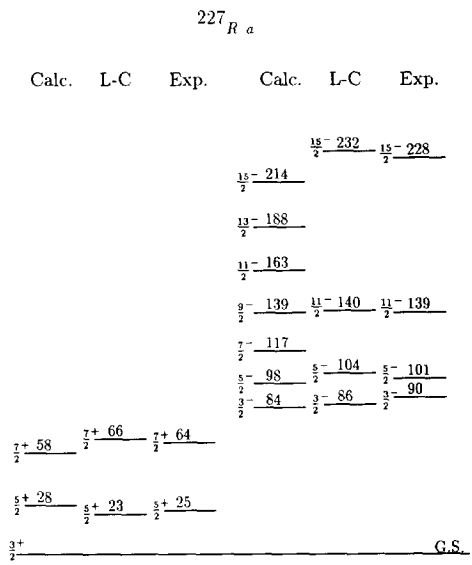

Fig. 29. Experimental [5] and calculated energy levels of ^{227}Ra in (keV). The theoretical energy levels obtained in the framework of the microscopic model by Leander and Chen (L–C) are taken from Ref. [5]. We are predicting the position of the $\frac{7}{2}^-$, $\frac{11}{2}^-$ and $\frac{13}{2}^+$ states for ^{227}Ra, for which the corresponding experimental observations are absent [5]. The positions of these levels are not discussed by Leander and Chen [5].

$$\mathcal{F}_0 = \frac{1}{6}\frac{\sum_{\lambda=2}^{N}(\lambda+1)\left(\beta_\lambda^0\right)^2}{\sum_{\lambda=2}^{N}\left(\beta_\lambda^0\right)^2/\lambda}. \tag{79}$$

Let us analyze the behavior of $R(I,L)$ as a function of spin I. The ratios of reduced probabilities $R(I,L)$ (74) for $L = 1,2,3$, calculated in our model, and experimental data for ^{226}Ra are presented in Table 3. The experimental data for $R(I,L)$ are extracted from analysis of the Coulomb excitation reaction in Ref. [27]. The values of $R(I,L)$ obtained in the rigid-rotor approximation are also presented in Table 3. The level scheme of ^{226}Ra is shown in Fig. 14.

The parameter $\mathcal{F}_0 = 1.62$ is evaluated by the method described above. The parameters of volume and surface stiffness, $J = 32.5$ MeV and $Q = 50$ MeV, needed for calculation of the PEDM, were taken from Refs. [7,11,14].

The result for $R(I,L)$ provided by the soft-rotator model are always greater and closer to experimental data than those, given by the rigid rotator.

The soft-rotator calculations for EL transitions indicate first the decrease of $R(I,L)$ at small I, and then its smooth growth with increasing I. In contrast, the rigid-rotator model predicts a slow decrease at all values of I (see Table 3). This tendency is confirmed by experimental data, but it is somewhat obscure in the cases of quadrupole and octupole transitions for which some experimental points deviate from such average behavior. The procedure of extraction of transition matrix elements from data on the

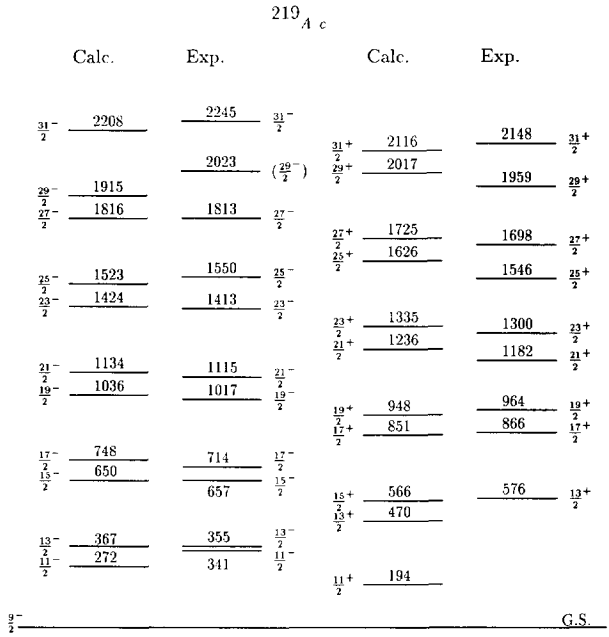

Fig. 30. Experimental [38] and calculated energy levels of ^{219}Ac in (keV). We are predicting the position of the $\frac{11}{2}^-$ and $\frac{13}{2}^+$ states for ^{219}Ac, for which the corresponding experimental observations are absent [38].

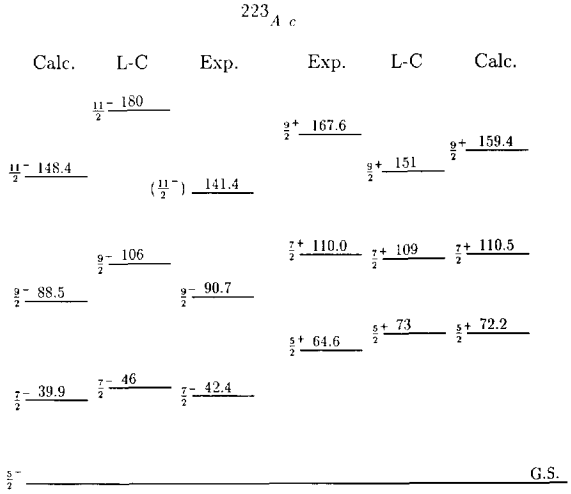

Fig. 31. Experimental [39] and calculated energy levels of ^{223}Ac in (keV). The theoretical energy levels obtained in the framework of the microscopic model by Leander and Chen (L–C) are taken from Ref. [5].

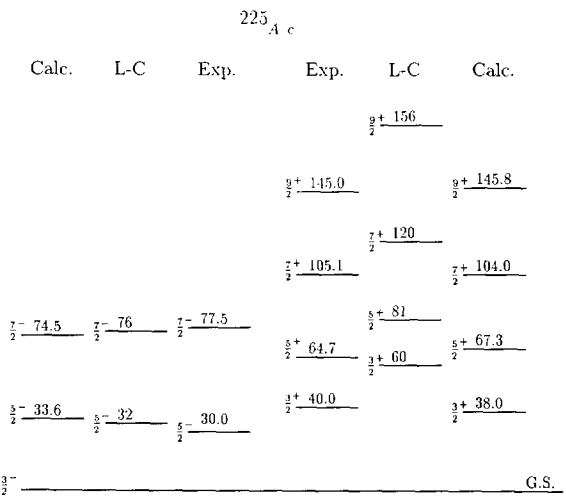

Fig. 32. Experimental [39] and calculated energy levels of ^{225}Ac in (keV). The theoretical energy levels obtained in the framework of the microscopic model by Leander and Chen (L–C) are taken from Ref. [5].

Table 3
Experimental [27] and theoretical values of the ratio $\mathcal{R}(I, L)$ with $L = 1, 2, 3$ for ^{226}Ra

Nucl.:	$L = 1$			$L = 2$			$L = 3$		
I	exp.	soft	rigid	exp.	soft	rigid	exp.	soft	rigid
0	$1.000^{+0.392}_{-0.392}$	1.000	1.000	$1.000^{+0.009}_{-0.009}$	1.000	1.000	$1.000^{+0.056}_{-0.056}$	1.000	1.000
1	$0.617^{+0.235}_{-0.235}$	0.676	0.667	$0.874^{+0.008}_{-0.009}$	0.643	0.600	$0.618^{+0.042}_{-0.036}$	0.591	0.571
2	$0.298^{+0.111}_{-0.111}$	0.623	0.600	$0.536^{+0.005}_{-0.005}$	0.533	0.514	$0.686^{+0.039}_{-0.039}$	0.491	0.476
3	$0.186^{+0.068}_{-0.068}$	0.608	0.571	$0.468^{+0.004}_{-0.004}$	0.533	0.476	$0.828^{+0.077}_{-0.077}$	0.471	0.433
4	$0.384^{+0.141}_{-0.141}$	0.621	0.556	$0.507^{+0.005}_{-0.005}$	0.500	0.455	$0.572^{+0.032}_{-0.034}$	0.443	0.408
5				$0.295^{+0.003}_{-0.003}$	0.524	0.441	$0.449^{+0.025}_{-0.025}$	0.455	0.392
6	$0.758^{+0.276}_{-0.276}$	0.663	0.538	$0.441^{+0.004}_{-0.004}$	0.511	0.431	$0.555^{+0.031}_{-0.033}$	0.443	0.380
7	$1.176^{+0.594}_{-0.594}$	0.672	0.533	$0.388^{+0.003}_{-0.004}$	0.543	0.424			
8	$1.355^{+0.497}_{-0.497}$	0.726	0.529	$0.402^{+0.004}_{-0.004}$	0.539	0.418	$0.244^{+0.032}_{-0.159}$	0.461	0.365
9	$1.535^{+0.605}_{-0.605}$	0.731	0.526	$0.472^{+0.005}_{-0.009}$	0.574	0.414			
10	$2.074^{+0.777}_{-0.777}$	0.801	0.524	$0.755^{+0.007}_{-0.008}$	0.577	0.410			
11	$2.130^{+0.878}_{-0.878}$	0.800	0.522	$0.851^{+0.018}_{-0.012}$	0.614	0.407			
12	$6.350^{+2.389}_{-2.389}$	0.883	0.520	$0.420^{+0.006}_{-0.004}$	0.621	0.404			
13	$6.259^{+2.587}_{-2.290}$	0.875	0.519	$0.682^{+0.071}_{-0.041}$	0.659	0.402			
14				$0.455^{+0.028}_{-0.007}$	0.669	0.400			
15	$3.903^{+1.468}_{-1.658}$	0.968	0.517						
16				$0.185^{+0.005}_{-0.004}$	0.669	0.400			

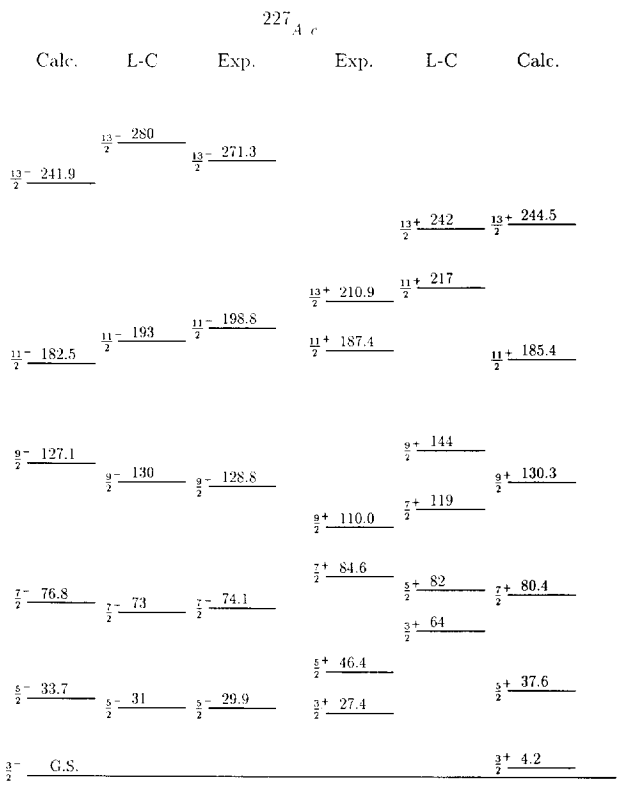

Fig. 33. Experimental [39] and calculated energy levels of ^{227}Ac in (keV). The theoretical energy levels obtained in the framework of the microscopic model by Leander and Chen (L–C) are taken from Ref. [5].

Coulomb excitation is not direct and unique [27]. We point out here that the values of the experimental matrix elements fluctuate strongly especially at large angular momenta in Ref. [27]. Therefore, if we do not consider some points strongly deviating from common tendencies in Table 3, then we can make the conclusion about good agreement between the experimental data and theory of soft rotator.

In Table 4 we compare the calculated and experimental branching ratios of the reduced probabilities for dipole and quadrupole transitions from the same level $W(I)$ for a number of radium and thorium isotopes. The values of the parameters $d_0^{\pm}$ are taken from Table 1 and β_2^0, β_3^0, ..., β_8^0 from Ref. [7]. The parameters $\mathcal{G}_1/\mathcal{G}_2$ in Table 4 are determined by the least-squares method minimizing the sum of relative deviations between the experimental and theoretical branching ratio $W(I)$ for each level of the considered nuclei.

The correlation between experimental and theoretical values of the branching ratio $W(I)$ is satisfactory for all the isotopes presented in Table 4.

Table 4 shows that the theoretical ratio of the reduced probabilities of dipole and quadrupole transitions, $W(I)$, increases slightly with the growth of the spin I. The same tendency is observed experimentally in ^{222}Th. In other isotopes the values $W(I)$

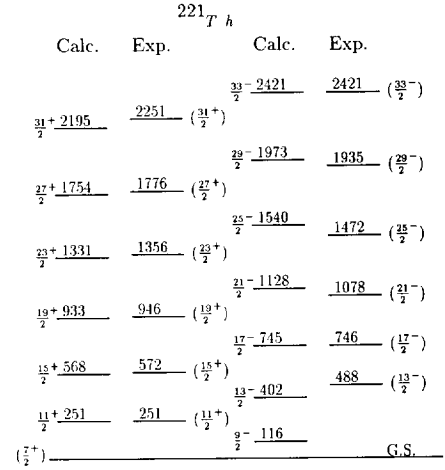

Fig. 34. Experimental [32] and calculated energy levels of ^{221}Th in (keV). We are predicting the position of the $\frac{9}{2}^-$ state for ^{221}Th, for which the corresponding experimental observations are absent [32].

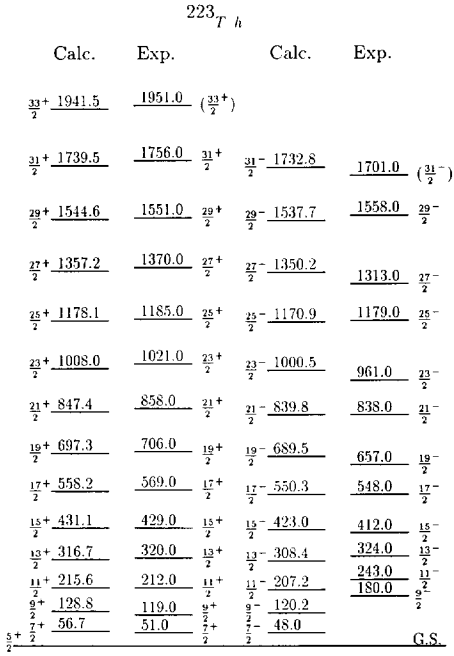

Fig. 35. Experimental [32] and calculated energy levels of ^{223}Th in (keV). We are predicting the position of the $\frac{7}{2}^-$ state for ^{223}Th, for which the corresponding experimental observations are absent [32].

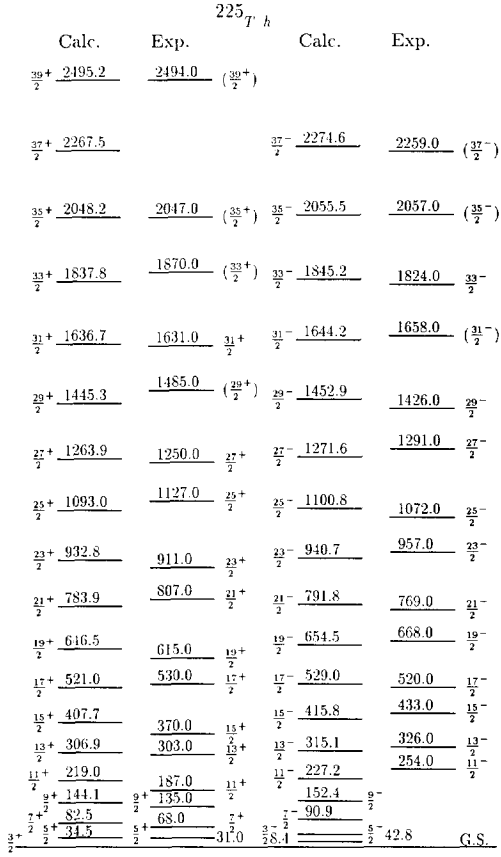

Fig. 36. Experimental [33] and calculated energy levels of ^{225}Th in (keV). We are predicting the position of the $\frac{3}{2}^-$, $\frac{5}{2}^-$, $\frac{7}{2}^-$ and $\frac{9}{2}^-$ states for ^{225}Th, for which the corresponding experimental observations are absent [33].

fluctuate strongly as a function of the spin.

In Table 4 we also present the results of calculation in which only quadrupole and octupole deformations are taken into account. These numerical results are much less than the experimental data. Therefore, the role of deformation of high multipolarity is very important for a correct estimation of the ratios of the reduced probabilities. Here we should remember that absolute values of the parameter $\mathcal{G}_{12}$ are always smaller than 1 (see also Refs. [14,15]). The growth of the branching ratio $W(I)$, when the deformations of higher multipolarities are taken into account, is associated with the corresponding increase of the PEDM, see Eq. (62).

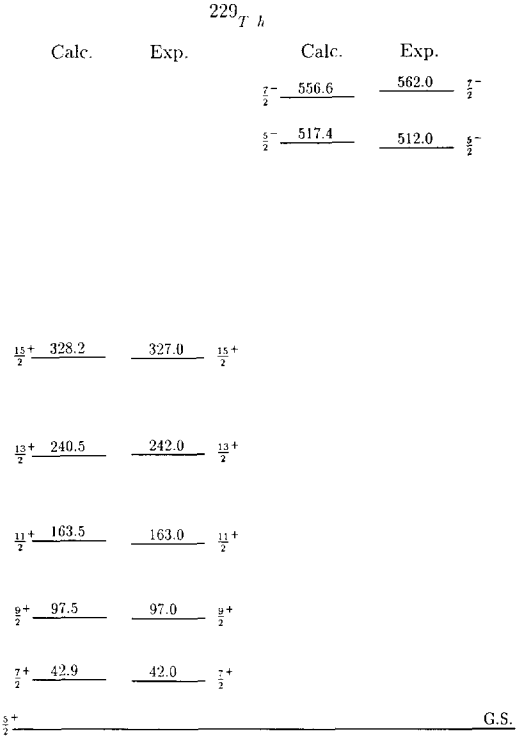

Fig. 37. Experimental [5] and calculated energy levels of ^{229}Th in (keV).

7. Conclusion

We constructed a generalized nonadiabatic model, analogous to that of Davydov and Chaban [45,46]. They dealt only with quadrupole deformations of even–even nuclei, while we considered a much more complicated case, when the equilibrium shape of the nucleus is defined by a few deformation parameters β_2^0, β_3^0, ..., β_N^0. Davydov and Chaban were able to calculate the energies only of the vibrational–rotational bands of positive parity; Williams and Davidson [49] only of the bands of negative parity. We have been starting from the very clear fact, that such nuclei with equilibrium deformations of odd multipolarity have two symmetric potential wells separated by a potential barrier, which enabled us to reproduce both bands simultaneously. We stress here that we fix only the energy of the nuclear ground state, but not the band-head of the opposite-parity band. These bands are associated with symmetric or antisymmetric combinations of the wave functions, describing vibrations in these two potential wells. A relative shift of the bands with opposite parity is due to tunneling under the potential barrier separating potential wells. An idea is also exploited that the power series for the potential energy in terms of deviations from minima of the potential energy β_λ^0 or $\beta_{\lambda'}^0$ must contain not only powers of $\beta_\lambda - \beta_\lambda^0$, but also their products $(\beta_\lambda - \beta_\lambda^0)^n(\beta_\lambda - \beta_\lambda^0)^m$,

Table 4
Experimental and theoretical values of the branching ratio $W(I)$ in units of 10^{-6} fm^{-2}

Nucl.:	^{218}Ra [18]			^{220}Ra [23]			^{220}Th [29]			^{222}Th [29]		
$\mathcal{F}_0$:		1.462	2.134		1.300	1.926		1.470	2.007		1.316	1.772
$\mathcal{G}_{12}$:		1.000	0.433		1.000	0.295		1.000	0.372		1.000	0.438
I	exp.	theor. $\beta_{2,3}$	theor. $\beta_{2,\ldots,8}$	exp.	theor. $\beta_{2,3}$	theor. $\beta_{2,\ldots,8}$	exp.	theor. $\beta_{2,3}$	theor. $\beta_{2,\ldots,8}$	exp.	theor. $\beta_{2,3}$	theor. $\beta_{2,\ldots,8}$
6	3.7	0.746	2.783				1.8	0.603	1.654	1.1	0.890	2.437
7	2.8	0.432	1.840				2.2	0.679	1.822	1.1	0.425	1.341
8	3.5	0.736	2.771	1.2	0.555	1.434	2.3	0.628	1.717	2.5	0.900	2.468
9	2.2	0.468	1.969				1.7	0.699	1.876	1.4	0.458	1.431
10	1.1	0.743	2.814	1.8	0.577	1.487	1.6	0.658	1.793	2.6	0.915	2.514
11	3.6	0.502	2.093	1.6	0.502	1.342	1.3	0.725	1.945	2.6	0.492	1.525
12	1.8	0.758	2.880	1.2	0.599	1.542				1.9	0.931	2.566
13	2.9	0.535	2.213	1.9	0.528	1.406				2.6	0.526	1.618
14	1.3	0.776	2.957	0.8	0.621	1.597				2.2	0.948	2.621
15	2.9	0.566	2.329	1.3	0.553	1.468				3.4	0.558	1.709
16												
17				2.1	0.577	1.529						

where $n, m = 0, 1, 2, \ldots$ and $n + m \geqslant 2$. Therefore, in the harmonic approximation there must exist uncoupled nuclear vibrations being mixtures of β_2, β_3, β_4, ...vibrations. In other words, pure quadrupole, octupole etc. vibrations can be met only occasionally. In the general case the nuclear potential energy has a complicated structure and its choice as in (22) is based only on our desire to solve the problem analytically. In principle, these solutions might be treated as a zero-order approximation and any additional terms of the potential energy might be taken into account as a perturbation.

In applications of the model we described only the ground-state band and the matched band of the opposite parity with the help of a very limited number of fitting parameters. It is worth noting that excited bands, built on the global $\widetilde{\beta}$ vibrations, must exactly repeat the main bands with $n = 0$. They need no additional parameters except for $\mathcal{F}_0$, which defines the band-head position. At the same time the description of the bands, built on excited angular vibrations, demands new parameters $\Delta^{\pm}$ or $d^{\pm}$ depending on the angular-phonon numbers ν. Choosing experimental data for comparison with calculation we have been taking either generally adopted levels of two bands of opposite parity or, in some cases, those with nearest energy to the calculated one. Sometimes there is a discrepancy between the model and experiment for low-lying levels of odd parity. In even–even isotopes the experimental data for the 1^- state are absent, owing to difficulties in its observation [58]. There are different opinions about its existence in nature. Here we assume that this level exists really in a sequence $1^-, 3^-, 5^-, \ldots$ with growing energies. And nevertheless our very simple model well describes the experimental data for most isotopes.

Acknowledgements

The authors are grateful to Prof. A.I. Levon for helpful discussions.

References

[1] S. Aberg, H. Flocard and W. Nazarewicz, Ann. Rev. Nucl. Part. Sci. 40 (1990) 439.
[2] I. Ahmad and P.A. Butler, Ann. Rev. Nucl. Part. Sci. 43 (1993), in press.
[3] R.K. Sheline, Phys. Rev. C 21 (1980) 1660.
[4] G.A. Leander, W. Nazarewicz, G.F. Bertsch and J. Dudek, Nucl. Phys. A 453 (1986) 58.
[5] G.A. Leander and Y.S. Chen, Phys. Rev. C 37 (1988) 2744.
[6] J.L. Egido and L.M. Robledo, Nucl. Phys. A 545 (1992) 589.
[7] P.A. Butler and W. Nazarewicz, Nucl. Phys. A 533 (1991) 249.
[8] V.M. Strutinsky, At. Energy 4 (1956) 150.
[9] C. Dorso, W. Myers and W. Swiatecki, Nucl. Phys. A 451 (1986) 189.
[10] W. Myers and W. Swiatecki, Nucl. Phys. A 531 (1991) 93.
[11] V.Yu. Denisov, Sov. J. Nucl. Phys. 49 (1989) 399.
[12] V.Yu. Denisov, Sov. J. Nucl. Phys. 55 (1992) 1478.
[13] A.Ya. Dzyublik and V.Yu. Denisov, Ukr. Phys. J. 37 (1992) 1770.
[14] A.Ya. Dzyublik and V.Yu. Denisov, Phys. At. Nucl. (former Sov. J. Nucl. Phys.) 56 (1993) 303.
[15] V.Yu. Denisov and A.Ya. Dzyublik, Phys. At. Nucl. (former Sov. J. Nucl. Phys.) 56 (1993) 477.
[16] V.Yu. Denisov, preprint LPN-Nantes-93-6 (1993).
[17] N. Roy, D.J. Decman, H. Kluge, K.H. Maier, A. Maj, C. Mittig, J. Fernandez-Niello, H. Puchta and F. Riess, Nucl. Phys. A 426 (1984) 379.
[18] J. Fernandez-Niello, H. Puchta, F. Riess and W. Trautmann, Nucl. Phys. A 391 (1982) 221.
[19] Y. Gono, T. Kohno, M. Sugawara, Y. Ishikawa and M. Fukuda, Nucl. Phys. A 459 (1986) 427.
[20] D. Cottle, M. Gai, J.F. Ennis, J.F. Shriner, D.A. Bromley, C.W. Beausang, L. Hildingsson, W.F. Piel, D.B. Fossan, J.W. Olness and E.K. Warburton, Phys. Rev. C 36 (1986) 2286.
[21] A.M.Y. El-Lawindy, J.D. Burrows, P.A. Butler, J.R. Cresswell, V. Holliday, G.D. Jones, R. Tanner, R. Wadsworth, D.L. Watson, K.A. Connell, C. Simpson, C. Lauterbach and J.R. Mines, J. Phys. G 13 (1987) 93.
[22] M. Wieland, J. Fernandez-Niello, F. Riess, M. Aïche, A. Chevallier, J. Chevalier, N. Schultz, J.C. Sens, Ch. Briancon, R. Kulessa and E. Ruchowska, Phys. Rev. 45 (1992) 1035.
[23] A. Celler, Ch. Briancon, J.S. Dionisio, A. Lefebvre, Ch. Vieu, J. Zylicz, R. Kulessa, C. Mitag, J. Fernandez-Niello, Ch. Lauterbach, H. Puchta and F. Riess, Nucl. Phys. A 432 (1985) 421.
[24] B. Ackermann, T. Bihn, P.A. Butler, V. Grafen, G. Günter, J.R. Hughes, G.D. Jones, Ch. Lauterbach, H.J. Mayer, M. Marten-Tölle, R. Tölle, R. Wadsworth, D.L. Watson and C.A. White, Z. Phys. 332 (1989) 375.
[25] E. Ruchowska, J. Zylicz, C.F. Liang, P. Paris and Ch. Briancon, J. Phys. G 18 (1992) 131.
[26] R.J. Poynter, P.A. Butler, N. Clakson, D. Cline, K.A. Connel, R.A. Cunningham, L. Goettig, T.H. Hoare, J.R. Hughes, N.S. Jarvis, G.D. Jones, S. Juutinen, S.M. Mullins, C.N. Pass, J. Simpson, R. Wadsworth, D.L. Watson and C.A. White, Phys. Lett. B 232 (1989) 447.
[27] H.J. Wollersheim, H. Emling, H. Grein, R. Kulessa, R.S. Simon, C. Fleischmann, J. de Boer, E. Hauber, C. Lauterbach, C. Schandera, P.A. Butler and T. Czosnyka, Nucl. Phys. A 556 (1993) 261.
[28] E. Ruchowska, W. Kurcewicz, N. Kaffell, T. Björnstad and G. Nyman, Nucl. Phys. A 383 (1982) 1.
[29] W. Bonin, H. Backe, M. Dahlinger, S. Glienke, D. Habs, E. Hanelt, E. Kankeleit and B. Schwartz, Z. Phys. A 322 (1985) 59.
[30] B. Schwartz, D. Habs, D. Schwalm, M. Dahlinger, E. Kankeleit, H. Folger and R.S. Simon, GSI Ann. Report, 1986, Darmstadt (1987) 31.
[31] P. Schuller, Ch. Lauterbach, Y.K. Agarwal, J. de Boer, K.P. Blume, P.A. Butler, K. Euler, Ch. Fleischmann, C. Günter, E. Hauber, H.J. Maier, M. Marten-Tölle, Ch. Schandera, R.S. Simon, R. Tölle and P. Zeyen, Phys. Lett. B 174 (1986) 241.
[32] M. Dahlinger, E. Kankeleit, D. Habs, D. Schwalm, B. Schwartz, R.S. Simon, J.D. Burrows and P.A. Butler, Nucl. Phys. A 484 (1988) 337.

[33] J.R. Hughes, R. Tölle, J. de Boer, P.A. Butler, C. Günter, V. Grafen, N. Gollwitzer, V.E. Holliday, G.D. Jones, C. Lauterbach, M. Marten-Tölle, S.M. Mullins, R.J. Poynter, R.S. Simon, N. Singh, R.J. Tanner, R. Wadsworth, D.L. Watson and C.A. White, Nucl. Phys. A 512 (1990) 275.
[34] W.R. Phillips, I. Ahmad, H. Emling, R. Holzmann, R.V.F. Jansens, T.-I. Khoo and M.W. Drigert, Phys. Rev. Lett. 57 (1986) 3257.
[35] W. Urban, G.A. Leander, W. Gast, J. Habbinghaus, A. Kramers-Flecken, K.P. Blum and H. Hubert, Phys. Lett. B 185 (1987) 331.
[36] W. Urban, R.M. Lieder, W. Gast, G. Habbinghaus, A. Krämer-Flecken, T. Morek, T. Rzaca-Urban, W. Nazarewicz and S.L. Tabor, Phys. Lett. B 200 (1988) 424.
[37] R.J. Poynter, P.A. Butler, G.D. Jones, R.J. Tanner, C.A. White, J.R. Hughes, S.M. Mullins, R. Wadsworth, D.L. Watson and J. Simpson, J. Phys. G 15 (1989) 449.
[38] S. Khazrouni, A. Chevallier, J. Chevallier, O. Helene, G. Ramanantsizehena and N. Schulz, Z. Phys. A 320 (1985) 535.
[39] R.K. Sheline, C.F. Liang and P. Paris, Int. J. Mod. Phys. A 5 (1990) 2821.
[40] M. Aïche, A. Chevallier, J. Chevallier, S. Huine, S. Khazrouni, N. Schulz and J.C. Sens, J. Phys. G 14 (1988) 1191.
[41] J. Kvasil, R.K. Sheline, I. Hrivnakova, C.F. Liang and P. Paris, Int. J. Mod. Phys. E 5 (1992) 845; C.F. Liang, P. Paris, J. Kvasil and R.K. Sheline, Phys. Rev. C 44 (1991) 676.
[42] J. de Boer, N. Gollwitzer, A. Lösch, H.J. Maier, H. Müller, M. Rohn, B. Ackermann, T. Bihn, V. Grafen, C. Günter, M. Marten-Tölle, N. Singh, R. Tölle, Z. Phys. 344 (1992) 41.
[43] C.M. Lederer and V.S. Shirley, eds., Table of isotopes, 7th ed. (Wiley, New York, 1978).
[44] A. Bohr and B. Mottelson, Nuclear structure, vol. 2 (Benjamin, New York, 1974).
[45] A.S. Davydov and A.A. Chaban, Nucl. Phys. 20 (1960) 499.
[46] A.S. Davydov, Excited states of atomic nuclei (Atomizdat, Moscow, 1967) in Russian.
[47] A.S. Davydov and V.I. Ovcharenko, Yad. Fiz. 3 (1966) 1011 [Sov. J. Nucl. Phys. 3 (1966), English translation].
[48] P.O. Lipas and J.P. Davidson, Nucl. Phys. 26 (1961) 80.
[49] S.A. Williams and J.P. Davidson, Canad. J. Phys. 40 (1962) 1423.
[50] D.P. Leper, Nucl. Phys. 50 (1964) 420.
[51] A.Ya. Dzyublik, Ukr. Phys. J. 16 (1971) 894.
[52] L.D. Landau and E.M. Lifshitz, Quantum mechanics, nonrelativistic theory (Nauka, Moscow, 1974) in Russian.
[53] M. Born and K. Huang, Dynamical theory of crystal lattices (Oxford Univ. Press, Oxford, 1954).
[54] P.V. Skorobogatov, Sov. J. Nucl. Phys. 15 (1972) 124.
[55] N.Ya. Wilenkin, Special functions and theory of group representations (Nauka, Moscow, 1965) in Russian.
[56] A.Ya. Dzyublik and I.E. Kashuba, Ukr. Phys. J. 31 (1986) 810.
[57] V.M. Strutinsky, Nucl. Phys. A 95 (1967) 420; A 122 (1968) 1.
[58] M. Wieland, J. Fernandez-Niello, B. von Fromberg, F. Riess, M. Aïche, A. Chevallier, J. Chevalier, N. Schultz, J.C. Sens, Ch. Briancon and E. Ruchowska, Phys. Rev. 46 (1992) 2628.